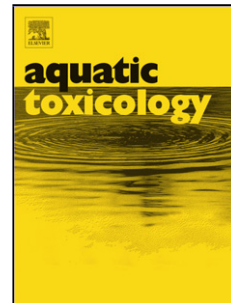


Journal Pre-proof

Impact of wastewater-borne nanoparticles of silver and titanium dioxide on the swimming behaviour and biochemical markers of *Daphnia magna*: an integrated approach

Victor Galhano, Sarah Hartmann, Marta S. Monteiro, Richard Zeumer, Darya Mozhayeva, Benedikt Steinhoff, Katharina Müller, Kirsten Prenzel, Jan Kunze, Klaus-Dieter Kuhnert, Holger Schönherr, Carsten Engelhard, Christian Schlechtriem, Susana Loureiro, Amadeu M.V.M. Soares, Klaudia Witte, Isabel Lopes



PII: S0166-445X(19)30808-2
DOI: <https://doi.org/10.1016/j.aquatox.2020.105404>
Reference: AQTOX 105404
To appear in: *Aquatic Toxicology*
Received Date: 2 October 2019
Revised Date: 3 January 2020
Accepted Date: 3 January 2020

Please cite this article as: Galhano V, Hartmann S, Monteiro MS, Zeumer R, Mozhayeva D, Steinhoff B, Müller K, Prenzel K, Kunze J, Kuhnert K-Dieter, Schönherr H, Engelhard C, Schlechtriem C, Loureiro S, Soares AMVM, Witte K, Lopes I, Impact of wastewater-borne nanoparticles of silver and titanium dioxide on the swimming behaviour and biochemical markers of *Daphnia magna*: an integrated approach, *Aquatic Toxicology* (2020), doi: <https://doi.org/10.1016/j.aquatox.2020.105404>

This is a PDF file of an article that has undergone enhancements after acceptance, such as the addition of a cover page and metadata, and formatting for readability, but it is not yet the definitive version of record. This version will undergo additional copyediting, typesetting and review before it is published in its final form, but we are providing this version to give early visibility of the article. Please note that, during the production process, errors may be discovered which could affect the content, and all legal disclaimers that apply to the journal pertain.

© 2020 Published by Elsevier.

Impact of wastewater-borne nanoparticles of silver and titanium dioxide on the swimming behaviour and biochemical markers of *Daphnia magna*: an integrated approach

Victor Galhano^{a1*}, Sarah Hartmann^{b1}, Marta S. Monteiro^a, Richard Zeumer^{c,d,e}, Darya Mozhayeva^f, Benedikt Steinhoff^{g,h}, Katharina Müller^b, Kirsten Prenzel^b, Jan Kunzeⁱ, Klaus-Dieter Kuhnertⁱ, Holger Schönherr^{g,h}, Carsten Engelhard^{f,h}, Christian Schlechtriem^{c,d,j}, Susana Loureiro^a, Amadeu M.V.M. Soares^a, Klaudia Witte^b, Isabel Lopes^a

^aDepartment of Biology and Centre for Environmental and Marine Studies (CESAM), University of Aveiro, Campus Universitário de Santiago, 3810-193 Aveiro, Portugal

^bResearch Group of Ecology and Behavioural Biology, Institute of Biology, Department of Chemistry-Biology, University of Siegen, Adolf-Reichwein-Strasse 2, Siegen 57076, Germany

^cFraunhofer Institute for Molecular Biology and Applied Ecology IME, Auf dem Aberg 1, Schmallenberg 57392, Germany

^dInstitute of Environmental Research (Biology V), RWTH Aachen University, Worringer Weg 1, Aachen 52074, Germany

^eFaculty of Agriculture/Environment/Chemistry, Dresden University of Applied Sciences, Friedrich-List-Platz 1, Dresden 01096, Germany

^fAnalytical Chemistry, Department of Chemistry-Biology, University of Siegen, Adolf-Reichwein-Strasse 2, Siegen 57076, Germany

^gPhysical Chemistry I, Department of Chemistry-Biology, University of Siegen, Adolf-Reichwein-Strasse 2, Siegen 57076, Germany

^hCenter of Micro- and Nanochemistry and Engineering (*Cμ*), University of Siegen, Adolf-Reichwein-Strasse 2, 57076 Siegen, Germany

ⁱInstitute of Real-time Learning Systems, Department of Electrical Engineering and Computer Science, University of Siegen, Hoelderlinstrasse, 3, Siegen 57076, Germany

^jEcotoxicology Work Group, Institute of Biology, Department of Chemistry-Biology, University of Siegen, Adolf-Reichwein-Strasse 2, Siegen 57076, Germany

***Corresponding author at:** Department of Biology & CESAM, University of Aveiro, Campus Universitário de Santiago, 3810-193 Aveiro, Portugal.

E-mail addresses: vgalhano@ua.pt (V. Galhano), hartmann@chemie-bio.uni-siegen.de (S. Hartmann), mmonteiro@ua.pt (M. Monteiro), richard.zeumer@htw-dresden.de (R. Zeumer), darya.mozhayeva@chemie.uni-siegen.de (D. Mozhayeva), steinhoff@chemie-bio.uni-siegen.de (B. Steinhoff), katharina3.mueller@student.uni-siegen.de (K. Müller), kirsten.prenzel@student.uni-siegen.de (K. Prenzel), jan.kunze@uni-siegen.de (J. Kunze), kuhnert@fb12.uni-siegen.de (K.-D. Kuhnert), schoenherr@chemie.uni-siegen.de (H. Schönherr), engelhard@chemie.uni-siegen.de (C. Engelhard), christian.slechtriem@ime.fraunhofer.de (C. Schlechtriem), sloureiro@ua.pt (S. Loureiro), asoares@ua.pt (A. Soares), witte@biologie.uni-siegen.de (K. Witte), ilopes@ua.pt (I. Lopes).

¹Both 1st authors.

HIGHLIGHTS:

- The effects of ASTM-dispersed and wastewater-borne nanoparticles of silver (NM-300K) and titanium dioxide (NM-105) were assessed in *Daphnia magna*.
- The behavioural and biochemical response-patterns are distinct after a 96-h exposition to wastewater-borne and ASTM-dispersed NPs.
- At the behaviour level, the most pronounced effects on the allocation time are obtained with ASTM-dispersed AgNPs.
- At the subcellular level, the wastewater-borne AgNPs are more toxic than wastewater-borne TiO₂NPs.

Abstract

Due to their widespread use, silver (Ag) and titanium dioxide (TiO₂) nanoparticles (NPs) are commonly discharged into aquatic environments via wastewater treatment plants. The study was aimed to assess the effects of wastewater-borne AgNPs (NM-300K; 15.5 ± 2.4 nm; 25-125 µg L⁻¹) and TiO₂NPs (NM-105; 23.1 ± 6.2 nm; 12.5-100 µg L⁻¹), from a laboratory-scale wastewater treatment plant, on *Daphnia magna*, at individual and subcellular level. For effect comparison, animals were also exposed to ASTM-dispersed NPs at the same nominal concentrations.

The behaviour of *D. magna* was evaluated through monitoring of swimming height and allocation time for preferred zones after 0 h and 96 h of exposure. Biochemical markers of neurotransmission, anaerobic metabolism, biotransformation, and oxidative stress were subsequently determined. No 96-h EC₅₀ (immobilization ≤ 4%) could be obtained with wastewater-borne NPs and ASTM-dispersed TiO₂NPs, whereas the ASTM-dispersed AgNPs resulted in an immobilization 96-h EC₅₀ of 113.8 µg L⁻¹. However, both wastewater-borne and ASTM-dispersed TiO₂NPs, at 12.5 µg L⁻¹, caused immediate (0 h) alterations on the swimming height. Allocation time analyses showed that animals exposed to ASTM-dispersed AgNPs spent more time on the surface and bottom at 0 h, and in the middle and bottom at 96 h. This pattern was observed neither with ASTM-dispersed TiO₂NPs nor with wastewater-borne AgNPs or TiO₂NPs. At the biochemical level, the more pronounced effects were observed with wastewater-borne

AgNPs (e.g. induction of lactate dehydrogenase and glutathione S-transferase activities, and inhibition of catalase activity).

This integrative approach showed that: (i) the behavioural and biochemical response-patterns were distinct in *D. magna* exposed to environmentally relevant concentrations of wastewater-borne and ASTM-dispersed NPs; (ii) the most pronounced effects on allocation time were induced by ASTM-dispersed AgNPs; and (iii) at the subcellular level, wastewater-borne AgNPs were more toxic than wastewater-borne TiO₂NPs. This study highlights the need for the assessment of the effects of wastewater-borne NPs under realistic exposure scenarios, since processes in wastewater treatment plants may influence their toxicity.

Keywords: AgNPs; Cladocera; Oxidative stress; TiO₂NPs; Vertical migration; Wastewater treatment plants

1. Introduction

Engineered nanomaterials (ENMs) are increasingly used in various applications and commercial products, ranging from common household items (e.g. textiles, paints, sunscreens, cosmetics) to novel medical technologies (Kahru and Ivask, 2013). However, important environmental concerns regarding ENMs still persist nowadays, because they can enter the environment from a multitude of sources either: (i) directly, e.g. during runoff of washed nanoparticles (NPs) from sunscreens and house wall paints after heavy rain (Kiser et al., 2009); or (ii) indirectly, e.g. through effluents from wastewater treatment plants (WWTPs) (Lazareva and Keller, 2014; OECD, 2016). Regardless of their provenience, the ENMs are likely to enter both surface water and groundwater systems, thereby posing risks to aquatic biota and affecting the drinking water resources (Gartiser et al., 2014; Georgantzopoulou et al., 2018). In this regard, the EU-2020 legislative framework entails restrictive effluent standards for protected areas and severe restrictions on WWTP-effluent properties, which can potentially contain ENMs (Lai et al., 2018; Svanström et al., 2014). Therefore, according to the precautionary principle adapted by the current legislation contemplated in the Registration, Evaluation, Authorisation and Restriction of Chemicals, and in the context of the continuous increase of the sustainable nanotechnology industry at the global scale, a consistent and well-founded prospective environmental risk assessment strategy for safe implementation of ENMs in wastewater

management programmes still needs to be adopted (Lai et al., 2018; Roco et al., 2011). Although few reports claim that there is no clear evidence of damage towards aquatic biota with regard to the current low discharge levels of ENMs (measured or measure-based predicted) (Coll et al., 2016), it is well accepted that there is a gap of knowledge regarding the fate and effect of wastewater-borne manufactured nanomaterials on dynamic and complex WWTP-associated environments. Effectively, despite the recommendations of international policies for a critical need of **environmental risk assessment** on wastewater-borne ENMs, comprehensive knowledge on their ecotoxicological effects on aquatic biota is still very poor.

Even though different types of NPs have been detected in receiving effluents from WWTPs (Brar et al., 2010; Kiser et al., 2009), their ecotoxicological effects on aquatic biota have been scarcely addressed in this matrix (Gartiser et al., 2014; Wu et al., 2018). So far, few studies (Georgantzopoulou et al., 2018; Hartmann et al., 2019; Kühr et al., 2018; Muth-Köhne et al., 2013) reported the toxicity effects of silver NPs (AgNPs) and titanium dioxide NPs (TiO₂NPs), two commonly used **ENMs**, in several manufactured products (Kahru and Ivask, 2013; Roco et al., 2011; Zhang et al., 2018), on aquatic biota and after passing through WWTP compartments. These findings indicated that, despite the very low concentrations (in the µg L⁻¹ range) found in WWTP effluents (Lazareva and Keller, 2014; Maurer-Jones et al., 2013), the so-called wastewater-borne NPs could be potentially very harmful to aquatic organisms (Muth-Köhne et al., 2013). The composition and properties of wastewater effluents show big differences and present additional substances compared to those of natural water, such as type and quantity of metal ions, composition of dissolved organic matter (DOM; with humic and fulvic acids), colloidal substances, electrolytes, and several types of soluble microbial products derived from the metabolism of the microbiome (Mahlalela et al., 2017; Zhou et al., 2015). Once present in influent, the NPs can undergo several transformation processes (*e.g.* dissolution, sulphidation, aggregation, coating with DOM, adsorption to biological surfaces, and deposition/sedimentation), which may ultimately influence their speciation in the effluent and, thereafter, affect their fate, transport, bioavailability and toxicity to aquatic organisms (Adam et al., 2018; Zhang et al., 2018). Therefore, in order to assess the toxicological effects of wastewater-borne AgNPs and TiO₂NPs on non-targeted biota, new approaches must be developed and optimized accordingly, taking into account the intrinsic complexity of these particular matrices.

Ecotoxicological tests with different model organisms have been recently performed to get insight into the toxicity mechanisms associated with AgNPs and TiO₂NPs present in WWTP effluents (Georgantzopoulou et al., 2018; Hartmann et al., 2019; Kühr et al., 2018; Muth-Köhne et al., 2013). Besides, the fate and ecotoxicity of both AgNPs and TiO₂NPs were already investigated in aquatic compartments at defined concentrations (Ribeiro et al., 2017; Sharma, 2009). Based on prospective models, predicted environmental concentrations (PECs) of NPs for several compartments in WWTPs, both in influents and effluents, are available. For example, in effluents, Maurer-Jones et al. (2013) summarized PECs of 0.0164-17 $\mu\text{g L}^{-1}$ and 1-100 $\mu\text{g L}^{-1}$ for AgNPs and TiO₂NPs, respectively. These values were subsequently updated for WWTP effluents from the EU countries by Sun et al. (2014), which specifically pointed to integer PECs of 0.17 ng L^{-1} and 16 $\mu\text{g L}^{-1}$ for AgNPs and TiO₂NPs, respectively.

Among the studies mentioned above, a few works on the environmental impact of AgNPs and TiO₂NPs from WWTPs on aquatic biota have been mainly focused on their toxicological effect at only one level of biological organisation, normally considering survival and growth as endpoints. To the best of knowledge of the authors, no studies are currently available regarding the toxicity of both types of wastewater-borne NPs through following a consistent and integrated approach at different levels of biological organisation. Therefore, since the responses at the lower level can act as early warning signals for the effects on higher level, the main objective of this study was to generate, integrate and add valuable knowledge on the toxicity evaluation profile of wastewater-borne AgNPs and TiO₂NPs, to the water flea *Daphnia magna*, a global keystone species of freshwater ecosystems, at both behavioural and biochemical level.

Specifically, this study was aimed at: (i) evaluating the toxicity of wastewater-borne effluents containing AgNPs (originally NM-300 K) and TiO₂NPs (originally NM-105) to the freshwater cladoceran *D. magna*; and (ii) infer on its toxicity through simple spiked media with the same original particles. This approach will be carried out through the assessment of behavioural (swimming height and allocation time) and biochemical (neurotransmission, anaerobic metabolism, biotransformation, and oxidative stress biomarkers) endpoints, in order to (a) elucidate the respective modes/mechanisms of action of each type of NPs by linking the effects at both levels of organisation, and (b) provide insight into and establish interrelationships between the early warning responses at the biochemical level to be translated at the behavioural level. This new combined

approach should, therefore, contribute to a better comprehension of the effects caused by NPs on aquatic organisms and provide input towards a more realistic risk assessment.

2. Materials and methods

2.1. Silver and titanium dioxide nanoparticles

The aqueous dispersions of AgNPs (test material: NM-300K) were obtained from the Organisation for Economic Co-operation and Development (OECD) Working Party on Manufactured Nanomaterials sponsorship programme. The dispersions of NM-300K NPs have a stated nominal silver (Ag) concentration of 10% (w/w), primary particle size of 15.5 ± 2.4 nm [measured in-house by transmission electron microscopy (TEM) in ASTM medium] and are stabilized with NM-300K DIS, a mixture of non-ionic dispersing agents containing 4% (w/v) of each polyoxyethylene glycerol trioleate (trade name: Tagat[®] TO) and polyoxyethylene (20) sorbitan monolaurate (trade name: Tween[®] 20). Also obtained from the OECD Working Party on Manufactured Nanomaterials programme, the NM-105 reference material was used for the preparation of the TiO₂NPs stock dispersions. Presented as a dry white powder, the uncoated TiO₂NPs consisted of anatase and rutile (86:14 ratio) individual particles with a primary particle size of 23.1 ± 6.2 nm (measured in-house by TEM in ASTM medium).

2.2. Lab-scale wastewater treatment plant (WWTP)

By following the OECD test guideline No. 303A (OECD, 2001), up to six units of a lab-scale WWTP (behrotest[®] Laboratory Sewage Plant KLD 4N, behr Labor-Technik GmbH, Düsseldorf, Germany) were set up and conducted as previously described (Hartmann et al., 2019). The details about the constitution and functioning of WWTP and the obtention of NP-containing effluents for exposure experiments (Section 2.4) are provided in the Materials and Methods section of the Supporting Information. In two independent experiments, namely 1A and 2A for AgNPs and TiO₂NPs, respectively (Table 1), the NPs were added to the influent at the denitrification reactor. The concentrations of NPs in the influent were chosen in order to achieve, after proper dilution, environmentally relevant concentrations in the obtained effluent, which may potentially result in quantifiable effects. In total, six and four WWTP units ran with AgNPs and TiO₂NPs, respectively, including the respective effluent controls without NPs. Concentrations of total Ag and total titanium (Ti) were measured in the collected

effluents after their passage through the WWTP units (Ag: after 26 days-d; Ti: directly after system operation). Inductively coupled plasma – mass spectrometry (ICP-MS) and inductively coupled plasma – optical emission spectrometry (ICP-OES) were used for the determination of total Ag and total Ti concentrations, respectively. The analytical protocols and main instrumental parameters are described in detail in the Supporting Information (Materials and Methods), including Table S1.

2.3. Test species and culture conditions

The freshwater crustacean *Daphnia magna* Strauss (clone V) was used as model species. Organisms were kept in permanent in-house breeding at $20 \pm 2^\circ\text{C}$ with a 16/8 h (light/dark) photoperiod, using 2 L glass beakers (pools of 30 adults per beaker), filled with 1.8 L of ASTM reconstituted hard water, and supplemented with vitamins (biotin, thiamine hydrochloride, cyanocobalamin) and selenium. The culture medium was renewed once a week and animals were fed daily with *Desmodesmus subspicatus*, with an amount of 0.2 mg C/*Daphnia*/day.

2.4. Exposure experiments

2.4.1. Controls and treatments

Three NP-free controls were used in exposure experiments (Table 1), namely an effluent control (EFF; in 1A and 2A with wastewater-borne NPs), an ASTM medium control (CT; in 1B and 2B with ASTM-dispersed NPs) and a dispersant agent control (DA; in 1B with ASTM-dispersed AgNPs).

For exposure experiments with wastewater-borne AgNPs (1A; Table 1) and wastewater-borne TiO₂NPs (2A; Table 1), the collected effluents from the model WWTP were manually shaken for 2 min to generate homogeneous dispersions, which served as stocks for further dilutions. Based on the total concentrations of NPs measured in the effluent, proper dilutions were performed with ASTM medium to achieve the respective nominal concentrations of 25-125 $\mu\text{g L}^{-1}$ of total Ag and 12.5-100 $\mu\text{g L}^{-1}$ of total Ti. The concentration range of AgNPs was chosen according to Völker et al. (2013a), which determined a nominal 48-h EC₅₀ (immobilization) of 121 $\mu\text{g L}^{-1}$ AgNPs in *D. magna*. The concentration range of TiO₂NPs was selected taking into account the nominal PECs of 1-100 $\mu\text{g L}^{-1}$ TiO₂NPs (Maurer-Jones et al., 2013). The dilution factors (parts of effluent

per parts of ASTM medium) and information about the preparation of effluent-related treatments are detailed in Table 1.

To compare the effects of wastewater-borne NPs with the effects of ASTM-dispersed NPs, exposures were also carried out in ASTM medium containing AgNPs or TiO₂NPs at the same nominal concentrations. These treatments were prepared in two additional experiments, namely 1B and 2B for ASTM-dispersed AgNPs and ASTM-dispersed TiO₂NPs, respectively (Table 1). In 1B, the original glass vial with AgNPs was sonicated in an ultrasonic bath (Bransonic 221 ultrasonic cleaner, Branson Ultrasonic, USA) for 10 minutes to disperse agglomerates and avoid air bubbles. Afterwards, the AgNPs were diluted to 1 g L⁻¹ of total Ag with ASTM medium. This dispersion served as basis for subsequent dilutions, in order to achieve the final NP concentrations in the test medium (Table 1). Also, in 1B, proportional dilutions were prepared with the dispersing agent to check for potential effects of the solubilizing agent in the treatments containing ASTM-dispersed AgNPs. For this purpose, the solutions were prepared by mixing the aqueous solution of NM-300K DIS in the ASTM medium at the same concentration used for the preparation of the highest AgNP concentration, *i.e.* 125 µg L⁻¹ of total Ag.

To obtain the nominal concentrations of ASTM-dispersed TiO₂NPs (2B; Table 1), the NP powder was dispersed in polypropylene vials containing ASTM medium (VWR International, Darmstadt, Germany) at 500 mg L⁻¹ of total Ti. A homogeneous dispersion was obtained afterwards by sonicating the stock in an ultrasonic homogenizer (Bandelin SONOPLUS HD2200, Berlin, Germany; 13 mm MS 72 horn, 40% amplitude) for 16 min. This dispersion served as basis for further dilutions in order to achieve the respective final concentrations of TiO₂NPs in the tested media (Table 1).

As a standard endpoint in ecotoxicity testing, the NP concentration that led to 50% immobilization after 96 h [96-h EC₅₀; greatest half-maximal effective concentration (OECD, 2004)] was derived whenever possible.

All treatments described above served as test media for the subsequent behavioural (section 2.4.2) and biochemical (section 2.4.3) assays.

2.4.2. Behavioural assays

The behavioural assays were performed in a temperature-controlled room (20 ± 2 °C) under constant conditions. Pools of randomly selected 10-day old animals (~3.1 ± 0.3 mm) were used. A 100 mL glass vessel (97 × 44 × 34.5 mm³; model type 740-OG,

Hellma Analytics, Müllheim, Germany) served as test vessel (Fig. S1, B-C). For each assay, five replicates per concentration plus controls, with ten organisms each, were tested. A computer vision system was used to monitor the swimming behaviour of *D. magna* in real-time (Kunze et al., 2016). Briefly, the animal's behaviour was recorded with a custom-built 2D-dimensional tracking system in a test chamber, which was completely covered with black polyvinyl chloride plates to avoid light (Fig. S1, A). To record movements of animals in darkness, a CVI STAR BL-LED backlight source (Stemmer Imaging AG, Puchheim, Germany), with a wavelength of 850 nm, was placed near the test vessel (Fig. S1, B-C). This background illumination was chosen because it cannot be seen by *D. magna*, thereby not affecting their motion. Contrary to the record of animals at visible light, the darkness set up, with only a single background light, presents the advantage of avoiding possible additional stress, phototaxis and/or resulting artefacts/biases.

Immediately before the behaviour assays, the glass vessel was filled up with 100 mL of the respective exposure treatment (Table 1). Then, adult animals were rapidly and carefully transferred to the vessel by means of a fine mesh to minimize stress and avoid media dilution. For each trial, animals were randomly selected from the four culture beakers and immediately placed inside the vessel. In order to minimize water movements within the vessel, a period of 10 min was accomplished before recording. Afterwards, the onset of recording (time point 0 h) was triggered by the operator and swimming behaviour was registered in real-time. The animals were not fed during the recording process and only those with continuous swimming behaviour were considered. A minimal threshold of 100 s was set in order to exclude reflections or crossings of/by organisms within analyses. The behaviour was recorded in the test vessel for 2 min [time period long enough to detect behavioural responses (Bownik, 2017, and references therein)]. The 2-min recording process was done at two precise time points, viz. immediately at the beginning of experiments (0 h), to measure the short-term effects of NPs on the behaviour, and after 96 h, to assess long-term responses. The 96 h exposure time was chosen because it was shown that *D. magna* exhibited an increased sensitivity to NPs during this period of time, as evaluated through the respective immobilization EC₅₀'s [e.g. for TiO₂NPs: 96-h EC₅₀ = 0.73 mg L⁻¹; 72-h EC₅₀ = 3.8 mg L⁻¹; Dabrunz et al. (2011)].

The average swimming height, i.e. the vertical path length (in mm), from the bottom to the top of the test vessel [an addition parameter that has been proven to provide a good feedback on the negative effects induced by the exposure of animals belonging to

the genus *Daphnia* to chemical substances, including NPs (Bownik, 2017)], and allocation time (defined as the time that animals spent in a specific zone within the test vessel; in s) were assessed as behaviour-related markers. For allocation time evaluation, the total volume of the test vessel (Fig. S1, B-C) was horizontally divided into three same-sized swimming zones, named 1 (top), 2 (centre) and 3 (bottom). Normally, zooplankton organisms belonging to the genus *Daphnia* present randomly swimming trajectories in defined volumes of water when stimuli (e.g. predator cues, matting, light) are absent, like in our experimental setup (Uttieri et al., 2004; Uttieri et al., 2005). Once organisms detect a chemical signal (e.g. dispersed NPs), their swimming behaviour become more coherent and deterministic, thus reflecting a change in the resulting trajectories (see e.g. Noss et al. (2013) for TiO₂NPs). These observations served as the rationale for the selection of the swimming zones within the test vessel, thereby assuming zone 2 as the preferred one. The pH, temperature and dissolved oxygen were monitored with a digital precision meter (WTW Multi 3430, WTW GmbH, Weilheim, Germany) in all treatments and respective controls, both directly after media preparation (0 h) and after 96 h (Table S2). All parameters fulfilled the criteria of the OECD test guideline No. 202 (OECD, 2004).

2.4.3. Biochemical assays

After the 96 h of exposure required for the behavioural assays, the animals were removed from the test vessel and appropriately maintained on ice until storage. For this purpose, the organisms in each replicate (N = 3-4; 9-10 animals per replicate; 14-d old) were pooled together to yield enough biomass for the determination of total protein content and biochemical markers. Aiming at a complete removal of NPs from the outer carapace of *D. magna*, each pool of organisms was carefully rinsed thrice with 0.1 M phosphate buffer saline (pH 7.4) to prevent potential bias caused by *in vitro* interactions. The organisms were then immediately transferred to 1.5 mL microtubes, filled with ice-cold 0.1 M phosphate buffer saline (pH 7.4) at 100 μ L organism⁻¹, snap-frozen in liquid nitrogen and stored at -80 °C until processing.

A battery of biochemical markers related to neurotransmission (acetylcholinesterase, AChE), anaerobic metabolism (lactate dehydrogenase, LDH), biotransformation (glutathione S-transferase, GST), and oxidative stress (catalase, CAT; lipid peroxidation, LPO) were subsequently determined. These biochemical markers were selected because published literature has already shown that they were affected in *D.*

magna exposed to NPs (see *e.g.* Klaper et al., 2009; Ulm et al., 2015). Samples were thawed on ice and homogenized with an ultrasonic homogenizer (Sonifier 250A, Branson Ultrasonics; pulse intensity and duration adjusted accordingly). An aliquot of 150 μL of the resulting homogenate was placed in a microtube with 4 μL 2,6-Di-*tert*-butyl-4-methylphenol for LPO determination. The remaining volume was centrifuged at 10,000 $\times g$ for 20 min at 4 °C to separate the **post-mitochondrial supernatant**. **This** fraction was divided into aliquots for the subsequent quantification of each enzymatic activity and further diluted in 0.1 M **phosphate buffer saline** (pH 7.4) whenever necessary. All reactions were performed in 96-wells microplates at 25 °C and determined spectrophotometrically in a microplate reader (Multiskan Spectrum, Thermo Fisher Scientific, Waltham, USA) by following the methodologies briefly described below.

The AChE activity was measured by using acetylthiocholine iodide as substrate, according to Ellman et al. (1961) and adapted to microplate by Guilhermino et al. (1996), through monitoring the absorbance (414 nm) of complexes formed by the thiol reagent 5,5'-dithiobis(2-nitrobenzoic acid) and thiocholine, every 20 s, during 5 min ($\epsilon_{414} = 1.36 \times 10^4 \text{ M}^{-1} \text{ cm}^{-1}$). The AChE activity was expressed as nmol of hydrolysed substrate per min per mg of protein. The LDH activity was evaluated by monitoring, at 340 nm (every 20 s, during 5 min), the decrease of NADH ($\epsilon_{340} = 6.3 \text{ mM}^{-1} \text{ cm}^{-1}$) due to its oxidation, as per Vassault (1983), adapted to microplate (Diamantino et al., 2001), and expressed as nmol of hydrolysed substrate per min per mg of protein. The GST activity was measured according to the method of Habig et al. (1974), adapted to microplate, and monitored every 20 s during 5 min at 340 nm; it was expressed as nmol of the conjugated substrate (2,4-dinitrochlorobenzene plus **reduced glutathione**) per min per mg protein ($\epsilon_{340} = 9.6 \times 10^3 \text{ M}^{-1} \text{ cm}^{-1}$). The CAT activity was assayed by following the decrease of absorbance at 240 nm due to H_2O_2 consumption ($\epsilon_{240} = 40 \text{ M}^{-1} \text{ cm}^{-1}$), recorded every 10 s during 2 min, and expressed as μmol of hydrolysed H_2O_2 per min per mg protein (Clairborne, 1985). The LPO levels were quantified according to the **thiobarbituric acid reactive substances** assay (Ohkawa et al., 1979), by measuring the amount of malondialdehyde-**thiobarbituric acid** complex ($\epsilon_{535} = 1.56 \times 10^5 \text{ M}^{-1} \text{ cm}^{-1}$), and expressed as nmol of hydrolysed **thiobarbituric acid reactive substances** per mg of protein. All biochemical marker measurements were repeated 2-4 times and normalized to protein concentration. Protein was determined at 595 nm (Bradford, 1976), with the Bio-Rad[®] dye-binding micro-assay method adapted for 96-well microplates. The bovine γ -globulin was used as standard.

All reagents for the determination of enzymatic activities, lipid peroxidation, and protein assays were of the highest available analytical grade quality ($\geq 99\%$) and were purchased from Merck KGaA (Darmstadt, Germany), with the exception of Bradford reagent (Bio-Rad, Munich, Germany). Ultra-pure water was prepared by using a Milli-Q modified academic water purification system (Merck KGaA, Darmstadt, Germany).

2.5. Characterisation of nanoparticles

Scanning transmission electron microscopy was performed on a FEI Talos F200X electron microscope with an acceleration voltage of 200 kV. A high-angle annular dark-field detector was used for a better contrast of NPs containing heavy elements (Ag and Ti) within an otherwise organic background. Energy-dispersive x-ray analysis was performed with a Super-X energy-dispersive x-ray detector to obtain spatially resolved elemental information. Fresh stock suspensions of AgNPs and TiO₂NPs at 100 $\mu\text{g L}^{-1}$ (nominal) were prepared in ASTM medium. At the beginning of the exposure (time point 0 h; see Section 2.4), two aliquots from stocks (40 mL each) were sampled, immediately frozen in liquid nitrogen in polypropylene centrifuge tubes (VWR International, Darmstadt, Germany) and stored at -20°C until use. The remaining dispersions (170 mL each) were transferred into sterile glass bottles and submitted to a 16/8 h (light/dark) photoperiod, at $20 \pm 2^\circ\text{C}$, for 96 h. Afterwards, the dispersions were homogenized by manual shaking and particles isolated from respective media via cloud point extraction (Hartmann et al., 2013). In parallel, previously frozen samples of ASTM medium and effluents (see Section 2.2) were thawed in a water bath at 30°C before preparation. All of the extracts proceeding from ASTM medium and effluent matrices were centrifuged onto an amorphous carbon-coated copper grid (200 mesh, Plano, Wetzlar, Germany). Organic residues were removed by depositing small droplets of absolute ethanol ($\geq 99.8\%$, VWR, Germany) on the copper grid, which were absorbed by underlying paper tissue.

The kinetic determination of particle size distribution was performed by single particle ICP-MS (spICP-MS) in ASTM medium aliquots withdrawn from a glass vessel in which organisms were exposed (Section 2.4). Contrary to TEM analysis, the medium in the test vessel was not homogenized before sampling in spICP-MS determinations because of the experimental design followed in the behavioural assays (see Section 2.4.2. for details). Accordingly, aliquots with a defined volume were taken from the middle zone

of the test vessel at 0, 3, 6, 12, 24, 48, 72 and 96 h. A model iCAP Qc (Thermo Fischer Instrument, Bremen, Germany) quadrupole ICP-MS was used. For characterisation of NM-300K NPs, the size calibration was done with 20 nm AgNPs (ECP1374, nanoComposix, San Diego, CA, USA), with a mean particle size of 18.5 ± 3.4 nm (TEM provided by the manufacturer). For characterisation of NM-105 NPs, the size calibration was done with TiO₂NPs (IoLiTec Ionic Liquids Technologies GmbH, Heilbronn, Germany), with a mean particle size of 41.5 ± 9.9 nm (in-house TEM measurements). Prior to spICP-MS measurements, samples were diluted with double distilled water in polypropylene centrifuge tubes (VWR International, Darmstadt, Germany) to ensure the detection of individual particles and were analysed right after dilution. A total consumption microflow DS-5 nebulizer (Teledyne CETAC Technologies, Omaha, NE, USA), operating at a self-aspiration rate of $\sim 5 \mu\text{L min}^{-1}$ and a low-volume spray chamber, was used for the analysis of AgNPs. A MicroFlow PFA-50 nebulizer (Thermo Fisher Scientific, Bremen, Germany), with a self-aspiration rate of $\sim 65 \mu\text{L min}^{-1}$ at 1 L min^{-1} of argon (according to the manufacturer instructions), and a Peltier-cooled cyclonic quartz spray chamber, held at $3 \text{ }^\circ\text{C}$, were used for the analysis of TiO₂NPs. An additional roughing pump (Sogevac SV40 BI, Leybold, Cologne, Germany) was connected to the instrument to decrease the interface pressure. Due to the principal limitation of the quadrupole mass analyser, only one isotope ($^{107}\text{Ag}^+$ or $^{49}\text{Ti}^+$) was monitored at a time to get continuous time-resolved measurements. A prototype data acquisition system (Streng and Engelhard, 2016), which was applied earlier for AgNP (Mozhayeva and Engelhard, 2017; Mozhayeva et al., 2017) and AuNP (Franze et al., 2017) characterization, was used to continuously acquire data with $5 \mu\text{s}$ time resolution to avoid signal artefacts often encountered in spICP-MS (Mozhayeva and Engelhard, 2020). The spICP-MS measurements were performed during 10 min and 3 min for AgNPs and TiO₂NPs, respectively. The main spICP-MS instrumental parameters are presented in Table S3.

2.6. Statistical analysis

Each data set of swimming height and biochemical markers was tested beforehand for normal distribution (Shapiro-Wilk test) and homoscedasticity (Brown-Forsythe test) prior to further analysis (all variables met the required assumptions). For swimming height analysis, a two-way analysis of variance (ANOVA), followed by Tukey's *post-hoc*

test was used to determine the interactive effect of each treatment (test medium with NPs, including controls) with the respective time point (0 or 96 h).

For the evaluation of immobilization, an appropriate dose-response model was adopted for each treatment and each particular time point. The model was selected based on Akaike's information criterion for each dataset of immobile organisms, thus allowing the calculation of the respective median effective concentrations (96-h EC₅₀s) by using the 'drc' extension package (Ritz et al., 2016).

For the evaluation of allocation time, the mean \pm standard error (SE) of animals distributed in each zone (1 – top; 2 – centre; and/or 3 – bottom) of the test vessel were determined. To analyse allocation time in the experiments, we used linear mixed effect in R (LMER) models with the *lmer* function of the 'lmerTest' package (Kuznetsova et al., 2017). The effect of each treatment assessed at each particular time point was analysed separately in a different model, with allocation time as the dependent variable (Kuznetsova et al., 2017). All models were computed to check if the allocation time of organisms followed a concentration-response pattern, taking into account all treatments and respective controls (EFF, DA or CT), wherefore the concentrations and controls were included into the models as numerical variables (fixed effects). Additionally, to test differences between DA and CT in the experiment with ASTM-dispersed AgNPs (Experiment 1B; Table 1), another model was performed, with allocation time as the dependent variable (as above), and DA and CT as categorical variables (fixed factors). The same settings of variables and factors as previously described were applied for two additional models, to compare the CT of Experiments 1B and 2B to the EFF of Experiments 1A and 2A (Table 1). The identity of animals nested in the test vessel was included as a random effect in all models. The verification of the assumptions of the models by visual inspection of residual plots (Q/Q, residuals against adjusted values and normality of residues) showed no clear deviations from normality and homoscedasticity. Conditional plots were made using the 'visreg' package (Breheny and Burchett, 2016).

For the analysis of biochemical markers, a one-way ANOVA followed by Dunnett's *post-hoc* test was used to check the differences between treatments and controls; the differences between means of the same concentration of NPs dispersed in different tested media or between controls were assessed with t-tests.

The analysis of swimming behaviour-related markers and calculation of 96-h EC₅₀ were done using R for Windows (version 3.2.4). All other analyses were performed with SigmaPlot for Windows, v. 14 (Systat Software, Inc., San Jose, CA, USA) and Statistica

64, v. 12 (StatSoft Inc., Tulsa, OK, USA). Results are expressed as mean \pm SE and α -level set at 0.05.

3. Results

3.1. Particle characterisation and size distribution

As revealed by TEM, the ASTM-dispersed AgNPs possessed a modal diameter of 15.5 ± 2.4 nm at 0 h, which did not change over time (15.6 ± 2.2 nm after 96 h; Fig. S2). The ASTM-dispersed TiO₂NPs formed agglomerates, comprising primary TiO₂ particles with a diameter of 23.1 ± 6.2 nm at 0 h, which also remained constant after 96 h (26.0 ± 5.8 nm; Fig. S3). The energy-dispersive x-ray analysis of wastewater-borne AgNPs showed that Ag was always co-localized with substantial amounts of sulphur, indicating a change in their chemical composition, from pristine Ag towards silver sulphide (Ag₂S). This was supported by the atomic Ag/S ratio of $\sim 2:1$ (Fig. 1A). It is therefore assumed that AgNPs were completely sulphidized in the effluent matrix. By contrast, the ASTM-dispersed AgNPs were not chemically affected over the 96-h period (Fig. 1B). In comparison to the sulphidized NPs, the amount of sulphur in ASTM-dispersed AgNPs was found to be substantially lower (atomic Ag/S ratio of $\sim 23:1$) and most likely stemmed from sulphate ions present in the ASTM medium (Fig. 1B).

For TiO₂NPs, the particles present in effluent and ASTM medium did not undergo any transformation because of their chemical inertness. In both matrices, the small amounts of sulphur detected by energy-dispersive x-ray analysis were exclusively attached to the organic matrix, as observed in the elemental maps (Fig. 2A, B). This was supported by the homogeneous distribution of sulphur on TiO₂ particles compared to locally concentrated signals of Ti and oxygen. Other elemental signals are either attributed contaminations (Si), spurious X-rays from the support grid (Cu), organic residues from the AgNP stabilizer and/or the cloud point extraction surfactant (C, O), or even residues (N, Na, Ca, Mg, P) from wastewater effluent or the ASTM medium (Fig. 1, 2).

The mean particle size evolution over time of ASTM-dispersed NPs obtained by spICP-MS is shown in Fig. 3. The size detection limit for both types of NPs was 10 nm (using Poisson statistics for data handling, with 5% false positive and 5% false negative error tolerances) (Mozhayeva and Engelhard, 2019). A Gaussian distribution was used for fitting particle size distributions. Due to the dispersing agent, all Ag particles remained

practically stable over 96 h in all dispersions and the mean particle size did not change to a high extent among all tested concentrations (Fig. 3A). Assuming a spherical shape of TiO₂ particles at all tested concentrations, the mean particle size decreased by $47.0 \pm 6.7\%$ until 12 h and then slightly decreased by up to $51.7 \pm 6.7\%$ of their initial average size after 96 h (in absolute: from 34 ± 1 nm at 0 h, to 17.2 ± 0.5 nm at 12 h, and to 15.6 ± 0.2 nm at 96 h; Fig. 3B).

3.2. Effects of wastewater-borne and ASTM-dispersed NPs

3.2.1. Effects on immobilization

The exposure to wastewater-borne AgNPs induced no effect on the immobilization of *D. magna* (Experiment 1A; Table S4). Though, the exposure of animals to ASTM-dispersed AgNPs resulted in a 96-h EC₅₀ for immobilization of $113.8 \mu\text{g L}^{-1}$ AgNPs (Experiment 1B; Table S4). The wastewater-borne TiO₂NPs (Experiment 2A; Table S4) and ASTM-dispersed TiO₂NPs (Experiment 2B; Table S4) caused low immobilization ($\leq 4\%$) to animals. Due to 100% immobilization of animals with $125 \mu\text{g L}^{-1}$ of ASTM-dispersed AgNPs at 96 h (Table S4), the respective treatment was not performed on the following behavioural and biochemical analyses.

3.2.2. Effects on behaviour

3.2.2.1. Swimming height

Concerning the effects of wastewater-borne or ASTM-dispersed AgNPs on the swimming height of *D. magna* (Fig. 4), a significant interaction was only observed between exposure duration and treatment ($p = 0.011$). Over time, *i.e.* from 0 to 96 h, there was a significant decrease in the swimming height of about 33, 44, and 40% in animals respectively exposed to DA, to $50 \mu\text{g L}^{-1}$ of wastewater-borne AgNPs, and to $75 \mu\text{g L}^{-1}$ of ASTM-dispersed AgNPs ($p < 0.05$).

Regarding the effects of wastewater-borne or ASTM-dispersed TiO₂NPs on the swimming height over time (Fig. 5), a significant interaction occurred between exposure duration and treatment factors ($p < 0.001$). Furthermore, significant differences were detected between the levels of each individual factor ($p < 0.001$).

At time 0 h, the animals exposed to $12.5 \mu\text{g L}^{-1}$ of wastewater-borne TiO₂NPs reduced swimming height to 39% compared to EFF; contrarily, the animals exposed to $12.5 \mu\text{g L}^{-1}$ of ASTM-dispersed TiO₂NPs showed an increase of 55% of swimming height

compared to CT ($p < 0.05$). Still, at 0 h, the swimming height of *D. magna* exposed to $12.5 \mu\text{g L}^{-1}$ of wastewater-borne TiO_2NPs was significantly lower than in those animals exposed to $12.5 \mu\text{g L}^{-1}$ of ASTM-dispersed TiO_2NPs ($p < 0.05$).

In general, there was a trend for reducing swimming height in organisms over time (from 0 to 96 h). Namely, this parameter was significantly reduced at 96 h by 38, 51, 17 and 29% in *D. magna* exposed to EFF, 25, 50 and $75 \mu\text{g L}^{-1}$ of wastewater-borne TiO_2NPs , respectively, and by 45 and 29% in animals exposed to 12.5 and $25 \mu\text{g L}^{-1}$ ASTM-dispersed TiO_2NPs , respectively.

3.2.2.2. Allocation time

In experiments with AgNPs, at both time points, *D. magna* exposed to DA spent more time in zone 1 (top) compared to animals in CT, (LMER, estimates: 12.43 (0 h), 44.38 (96 h); SE: 5.47 (0 h), 7.00 (96 h); t -value: 2.27 (0 h), 6.34 (96 h); $p \leq 0.03$; Table S5, Fig. 6A, B). At both time points, animals in EFF spent more time in zone 1 (LMER, estimates: 17.80 (0 h), 22.67 (96 h); SE: 6.69 (0 h), 9.08 (96 h); t -value: 2.66 (0 h), 2.50 (96 h); $p \leq 0.02$), and zone 3 (LMER, estimates: 16.97 (0 h), 10.50 (96 h); SE: 5.37 (0 h), 4.05 (96 h); t -value: 3.16 (0 h), 2.59 (96 h); $p \leq 0.01$) compared to animals in CT (Table S5; Fig. 6C, D).

The allocation time per zone of *D. magna* was not affected by wastewater-borne AgNPs at both time points [LMER, $p > 0.05$ (slope of each model)]; Table S5, Fig. 6E, F]. Notwithstanding, at 0 h, animals treated with ASTM-dispersed AgNPs spent more time in zone 1 (LMER, estimate: 3.63, SE: 1.27, t -value: 2.86, $p < 0.005$) and zone 3 (LMER, estimate: 2.59, SE: 0.98, t -value: 2.63, $p = 0.009$), and less time in zone 2 (LMER, estimate: -2.23, SE: 0.78, t -value: -2.87, $p = 0.004$) (Table S5; Fig. 6G). At 96 h, animals treated with ASTM-dispersed AgNPs spent more time in zone 2 (LMER, estimate: 3.76, SE: 1.38, t -value: 2.72, $p = 0.006$) and zone 3 (LMER, estimate: 3.29, SE: 0.44, t -value: 7.40, $p < 0.001$), and less time in zone 1 (LMER, estimate: -8.85, SE: 1.60, t -value: -5.53, $p < 0.001$) (Table S5; Fig. 6H).

The effects of TiO_2NPs on the allocation time of *D. magna* are depicted in Fig. 7. At 0 h, compared to CT, the EFF exposed animals spent more time in zone 3 (LMER, estimate: 22.05, SE: 3.16, t -value: 6.98, $p < 0.001$) and less time in zone 2 (LMER, estimate: -11.10, SE: 5.18, t -value: -2.15, $p = 0.034$; Table S5; Fig. 7A), and animals exposed to increasing concentrations of wastewater-borne TiO_2NPs spent less time in

zone 2 (LMER, estimate: -1.82, SE: 0.92, t -value: -1.99, $p = 0.047$). At 96 h, compared to CT, the EFF exposed animals spent less time in zone 1 (LMER, estimate: -15.70, SE: 7.32, t -value: -2.15, $p = 0.034$) and more time in zone 3 (LMER, estimate: 15.39, SE: 2.38, t -value: 6.47, $p < 0.001$) and animals spent more time in zone 1 (LMER, estimate: 32.00, SE: 3.78, t -value: 8.47, $p < 0.001$) and less time in zone 3 (LMER, estimate: -0.76, SE: 0.32, t -value: -2.40, $p = 0.017$) with increasing concentrations of wastewater-borne TiO₂NPs. In a different way, at 0 h, animals treated with increasing concentrations of ASTM-dispersed TiO₂NPs spent more time in zone 1 (LMER, estimate: 3.36, SE: 1.28, t -value: 2.63, $p < 0.001$) and less time in zone 2 (LMER, estimate: -3.90, SE: 0.81, t -value: -4.81, $p < 0.001$) (Table S5; Fig. 7E). At 96 h, with increasing concentrations of ASTM-dispersed TiO₂NPs, animals spent less time (LMER, estimate: -4.72, SE: 0.96, t -value: -4.90, $p < 0.001$) and more time (LMER, estimate: 5.67, SE: 0.83, t -value: 6.69, $p < 0.001$) in zones 2 and 3, respectively (Table S5; Fig. 7F).

3.2.3. Effects on biochemical markers

Compared to CT exposed *D. magna*, the DA exposed animals respectively showed a significant reduction of 37 and 21% of AChE and GST activities, and an increase of 33% of LDH activity ($p \leq 0.03$; Fig. 8). Compared to CT exposed organisms, the CAT activity significantly increased by 32 and 229% in EFF exposed animals used in AgNPs and TiO₂NPs experiments, respectively ($p \leq 0.02$; Fig. 8G, H). Besides, in TiO₂NP experiments, the EFF exposure caused a decrease of 64% and an increment of 44% on AChE and GST activities, respectively ($p = 0.01$; Fig. 8B, F).

In experiments with AgNPs, the AChE was only affected by the 75 $\mu\text{g L}^{-1}$ exposure to wastewater-borne AgNPs and the respective activity decreased 35% ($p = 0.03$; Fig. 8A). The AChE activity was 25% higher in 100 $\mu\text{g L}^{-1}$ of wastewater-borne AgNPs compared to ASTM-dispersed AgNPs at the same tested concentration ($p = 0.01$; Fig. 8A). Compared to EFF, the animals exposed to wastewater-borne AgNPs presented an increase of LDH activity of 129 and 180% at 50 and 125 $\mu\text{g L}^{-1}$, respectively ($p < 0.001$; Fig. 8C). Compared to *D. magna* exposed to ASTM-dispersed AgNPs at the same concentrations, the animals treated with 25 and 50 $\mu\text{g L}^{-1}$ of wastewater-borne AgNPs presented a higher LDH activity of 26 and 48%, respectively ($p = 0.01$; Fig. 8C). Compared to EFF exposed *D. magna*, there was an increase of GST activity of 120% in animals exposed to 100 $\mu\text{g L}^{-1}$ of wastewater-borne AgNPs ($p = 0.01$; Fig. 8E).

Furthermore, the GST activity was 19% higher at 100 $\mu\text{g L}^{-1}$ of wastewater-borne AgNPs compared to ASTM-dispersed AgNPs at the same concentration ($p = 0.01$; Fig. 8E). Compared to controls, organisms exposed to wastewater-borne AgNPs showed a reduction on CAT activity of 63, 69 and 65% with 25, 50 and 75 $\mu\text{g L}^{-1}$ AgNPs, respectively ($p \leq 0.01$; Fig. 8G). Besides, the CAT activity was 14 and 40% higher in organisms respectively exposed to 25 and 100 $\mu\text{g L}^{-1}$ of wastewater-borne AgNPs **comparatively** to organisms exposed to ASTM-dispersed AgNPs at identical concentrations ($p \leq 0.03$; Fig. 8G). **Animals** exposed to 75 $\mu\text{g L}^{-1}$ of wastewater-borne AgNPs presented 22% higher LPO levels than **animals** exposed to ASTM-dispersed AgNPs at the same concentration ($p = 0.03$; Fig. 8I).

In experiments with wastewater-borne TiO_2NPs , the only concentration responsible for a significant effect on AChE activity of ***D. magna*** was the highest tested (100 $\mu\text{g L}^{-1}$), and the respective value raised by 297% compared to EFF ($p = 0.001$; Fig. 8B). On the contrary, the AChE activity was reduced by 36 and 34% at 12.5 and 25 $\mu\text{g L}^{-1}$ of ASTM-dispersed TiO_2NPs , respectively ($p \leq 0.03$; Fig. 8B). Organisms exposed to 50 $\mu\text{g L}^{-1}$ of wastewater-borne TiO_2NPs presented a decrease on AChE activity of 68% compared to those exposed to ASTM-dispersed NPs at the same concentration ($p = 0.002$; Fig. 8B). The LDH activity was 118% lower in ***D. magna*** exposed to 100 $\mu\text{g L}^{-1}$ of wastewater-borne TiO_2NPs compared to animals exposed to ASTM-dispersed TiO_2NPs at the same concentration ($p = 0.04$; Fig. 8D). The only significant effect of wastewater-borne TiO_2NPs on GST was achieved at 25 $\mu\text{g L}^{-1}$, which caused a reduction of 49% on the respective activity ($p = 0.006$; Fig. 8F). Although wastewater-borne TiO_2NPs caused no significant effects on ***Daphnia's*** CAT, 12.5 $\mu\text{g L}^{-1}$ of ASTM-dispersed TiO_2NPs **led to** an increase of 449% of **its** activity ($p = 0.03$; Fig. 8H). At last, 25 $\mu\text{g L}^{-1}$ of ASTM-dispersed TiO_2NPs was the only **treatment** responsible for a significant change of the LPO levels in ***D. magna***, with a 52% reduction below controls ($p = 0.001$; Fig. 8J).

4. Discussion

In this study, we investigated the effects of environmentally relevant concentrations of wastewater-borne AgNPs and TiO_2NPs on behavioural and biochemical markers of *D. magna* in comparison to effects induced by the same type of NPs dispersed in ASTM medium.

4.1. Size characterisation of NPs

As shown by TEM and spICP-MS, the average size of Ag particles was stable over the exposure time, while for TiO₂NPs a decrease in the primary particle size occurred over time for all tested concentrations. These results are different from Jacobasch et al. (2014), which observed a rapid increase of particle size with increasing concentrations (from 1.19 to 6 mg L⁻¹; nominal) of TiO₂NPs (Evonik Aeroxide[®] P25; anatase-rutile, 21 nm) immediately upon dispersion in ElenDt M4 medium. Possible explanations for such a difference may be related to the different sampling procedures adopted and the media used in both studies. In the present work, the decrease of TiO₂ particle size after 12 h can be explained by the absence of a proper dispersing agent, with probable sedimentation of the formed TiO₂ agglomerates. It is worth mentioning that the aqueous samples for spICP-MS analysis were withdrawn from the middle of the water column to avoid a possible resuspension of the settled agglomerates. Notwithstanding, the primary particle size of TiO₂NPs determined by TEM was relatively constant over the 96-h period. This can be explained by the overall lower number of TiO₂ particles (compared to Ag particles) analysed by TEM, which most likely had an impact on the accuracy of particle size distribution determination, thus causing a minor deviation in their modal value over time. The diameter of TiO₂ particles represents the equivalent circle diameter since these particles are irregularly shaped within the agglomerates. Still, the different findings obtained with both analytical techniques herein applied could be explained by different sampling procedures in different media. Effectively, TEM samples were obtained from homogenized dispersions and therefore all particles and agglomerates present in suspension were considered for analysis. This contrasts with the sampling procedure adopted in spICP-MS analysis, *i.e.* without homogenization. Most likely, the agglomeration had already occurred in the medium as well as during the sampling deposition (as a drying artefact), which might have compromised the primary particle size analysis to a certain degree. In summary, the effects of both types of NPs described below cannot be simply explained by the variation of particle size distribution over time.

4.2. Effects on immobilization

The immobilization 96-h EC₅₀ for *D. magna* exposed to ASTM-dispersed AgNPs was 113.8 µg L⁻¹ of nominal Ag, whereas no immobilization was observed in other treatments. This value is in accordance with Völker et al. (2013a), who obtained an

immobilization 48-h EC₅₀ of 121 µg L⁻¹ (nominal) with AgNPs (NM-300K) dispersed in M4 medium. However, Muth-Köhne et al. (2013) reported that 0.7 and 5.5 mg L⁻¹ (nominal) of wastewater-borne AgNPs induced toxicity to 48 h-post-fertilized zebrafish (*Danio rerio*) larvae. Effectively, we found that wastewater-borne AgNPs did not affect mobility in *D. magna*, which is most likely explained by chemical transformations of AgNPs during the WWTP processing. The obtained scanning transmission electron microscopy images showed that AgNPs were sulphidized to Ag₂S to a great extent after their passage through the WWTP compartments. It is recognized that one important mode of action of AgNPs is the release of Ag⁺ from the surface of particles, which is toxic to aquatic organisms upon uptake (Ratte, 1999; Völker et al, 2013b). The Ag₂S has low water solubility [solubility product (K_{sp}) = 6×10^{-51} M³, at 25 °C], thus resulting in reduced bioavailability and toxicity of the AgNPs after sulphidation and/or complexation with other effluent ligands (Kaegi et al., 2011; Ratte, 1999). Our results are in agreement with Georgantzopoulou et al. (2018) and Hartmann et al. (2019), who showed that environmentally relevant concentrations of wastewater-borne AgNPs caused a significant reduction of toxicity in acute (48 h) and chronic (21 d) exposure experiments with *D. magna*, respectively. Irrespective of their dissolution capacity and the negative impact at the biochemical level, the assumption that wastewater-borne AgNPs are probably associated with the effluent solids that settled on the bottom of the test vessel in the form of precipitates (with reduction of direct exposure and ingestion by animals), should also be considered.

Regarding the effects of TiO₂NPs on *D. magna* immobilization, Lovern and Klaper (2006) reported a nominal 48-h EC₅₀ of 5.5 mg L⁻¹ TiO₂NPs, while Dabrunz et al. (2011) found a lower nominal EC₅₀ of 0.73 mg L⁻¹ TiO₂NPs with a 96-h test duration. However, the effects of such high concentrations were not considered herein, since experimental designs were based on available PECs (Maurer-Jones et al., 2013). Hartmann et al. (2019) found that 25-100 µg L⁻¹ (nominal) of wastewater-borne and ASTM-dispersed TiO₂NPs did not affect *D. magna* reproduction in up to six generations. In our study, the high mobility of animals exposed to wastewater-borne TiO₂NPs could be justified by the absence of transformation processes of the TiO₂ particles during their passage throughout the WWTP compartments. This was confirmed by scanning transmission electron microscopy analysis. On average, ~ 97% of engineered TiO₂NPs are released into surface waters in the non-transformed form and the only known

transformation process that occurred during the wastewater treatment is the formation of calcium titanate (Adam et al., 2018).

4.3. Effects of the dispersing agent

In our study, the AgNPs were sterically stabilized with a lipophilic mixture of two non-ionic synthetic dispersants in order to improve the dispersibility of particles, thereby preventing their settling and agglomeration. It is known that dispersing agents may increase NP toxicity, mainly through improved dispersibility, promoting the interaction between NPs and cell surfaces (Deng et al., 2017; Handy et al., 2012). Effectively, dispersing agents with lipophilic properties can interact with the lipid bilayer of cell membranes, thereby facilitating unintentional entry of NPs into cells (Deng et al., 2017; Handy et al., 2012). Our results support the evidence of DA toxicity to *D. magna*, since, after 96 h, the allocation time of DA exposed animals was affected in the three zones of the test vessel, being particularly evident at the top, thus indicating an avoidance response. Furthermore, the lipophilic mixture of surfactants was probably responsible for the induced effects, not only at the individual level but also at the biochemical level, since the DA caused inhibition of both AChE and GST activities, and induction of LDH activity. Considering other studies, 10 $\mu\text{g L}^{-1}$ of the same dispersing agent mixture caused no significant effects on length, survival rate and body burden of the freshwater amphipod *Hyaella azteca* (Kühr et al., 2018). In addition, Pettersson et al. (2000) confirmed that some non-ionic surfactants (26 detergents and 5 softeners) caused acute (48 h) toxicity to *D. magna*.

4.4. Effects of the effluent

The results of EFF at individual and biochemical level suggest that the background effluent used in TiO₂NP experiments induced neurotoxicity and oxidative stress in exposed animals. In *D. magna* subjected to this type of effluents, the neurotoxicological responses obtained at the biochemical level had also implications at the individual level, since the allocation time at the bottom of the vessel was significantly reduced over time.

It is well accepted that WWTP effluents comprise a complex mixture of substances which include, among others, soluble microbial products derived from the metabolism of different types of bacteria consortia normally present in synthetic sewage,

various types of DOM, colloidal substances, pharmaceutical products and further potentially harmful contaminants not eliminated by WWTPs (Kim and Farnazo, 2017; Mahlalela et al., 2017; Ren et al., 2017; Zhou et al., 2015). This amalgam of compounds was probably responsible for the observed effects of the EFF. Furthermore, the different ages of effluents at the beginning of the exposure assays (4-week and 3-month in AgNP and TiO₂NP experiments, respectively) may also have contributed to the different observed toxicity effects. It has been shown that ageing and properties of the exposure matrix may change not only its intrinsic toxicity but also the respective NP-associated toxicity (Cupi et al., 2015; Seitz et al., 2015). Consequently, the obtained effects caused by all NP-containing treatments at both behavioural and biochemical level should be interpreted in the light of the effect range of the respective background effluents.

4.5. Behavioural effects of wastewater-borne and ASTM-dispersed NPs

Regarding performed behavioural analyses, the swimming height of *D. magna* was neither affected by wastewater-borne AgNPs nor by ASTM-dispersed AgNPs. At 0 h, the exposure of *D. magna* to TiO₂NPs led to higher swimming heights, thus showing an immediate response of animals to this type of NPs. Pokhrel and Dubey (2012) showed that vertical migration of *D. magna* was not affected by 2 µg L⁻¹ of citrate-capped AgNPs (55.9 ± 14.6 nm), but the combination of citrate-AgNPs and a predator cue (dragonfly nymph, *Anax junius*) led to a significant vertical upward response compared to the predator treatment alone.

Considering the allocation time as endpoint, the swimming behaviour of *D. magna* was not affected by wastewater-borne AgNPs. On the other hand, animals exposed to ASTM-dispersed AgNPs spent more time at the top and at the bottom of the test vessel, which is in accordance with the obtained results for immobilization. The lack of changes in allocation time with wastewater-borne AgNPs could be justified by chemical transformations of AgNPs into other lesser toxic species (e.g. Ag₂S) in the effluent (Kaegi et al., 2011). Despite the absence of effects at the individual level, a significant inhibition of AChE activity was observed with 75 µg L⁻¹ of wastewater-borne AgNPs.

The irregular swimming behaviour of animals exposed to ASTM-dispersed AgNPs, could be indicative of the impairment of the nervous system with a consequent

loss of orientation. Poynton et al. (2012) showed that 10-day old *D. magna* exposed to AgNO₃ presented a downregulation of several gene sets involved in nervous system function, locomotion, behaviour and developmental processes. In agreement with these findings, important downregulated mechanisms related to the nervous system functioning were probably disturbed at the tested concentrations of ASTM-dispersed AgNPs, thus contributing to the abnormal swimming behaviour. Nevertheless, such mechanisms are not directly related to AChE, since no alterations in the activity of this enzyme were observed at all tested concentrations of ASTM-dispersed AgNPs. Besides, the increased tendency of the animals to swim towards the vessel surface at increasing concentrations of ASTM-dispersed AgNPs, at 0 h, may be interpreted as a rapid avoidance response probably based on a chemoreception mechanism. However, this response was lost after 96 h, probably due to a sedimentation process of the NPs or a yet unknown adaptation process. A similar avoidance behaviour was already observed in the freshwater snail *Physa acuta* exposed to 30 µg L⁻¹ of carboxy-functionalized AgNPs (1-10 nm) (Justice and Bernot, 2014).

The effects of TiO₂NPs on *D. magna* behaviour were studied by Noss et al. (2013), which found a concentration-dependent aggregation of animals in the central region of a vessel immediately upon exposure to 1, 5 and 20 mg L⁻¹ of TiO₂NPs (Evonik Aeroxide® P25; anatase-rutile, 21 nm). This aggregation phenomenon was interpreted as a kind of swarming behaviour, a well-known response of *Daphnia sp.* towards predator cues, abiotic factors, and neuro-active drugs (Čolović et al., 2013; Noss et al., 2013; Szulkin et al., 2006). However, Noss et al. (2013) also noticed that the swarming behaviour of TiO₂NP exposed animals disappeared after 24 h at all tested concentrations. In contrast, the daphnid's swarms of our study immediately exposed to wastewater-borne and ASTM-dispersed TiO₂NPs spent less time in the centre of the vessel. Still, this response was lost after 96 h with wastewater-borne TiO₂NPs but it was maintained with ASTM-dispersed TiO₂NPs. Since TiO₂NPs are rarely transformed during WWTP processing (Adam et al., 2018), a similar behavioural response would be expected in both TiO₂NP containing matrices which did not effectively occur, thus indicating that the two distinct matrices led to distinct effects over time. Despite these observations and taking into account the available literature (Sun et al., 2014), this is the first study which shows that environmentally relevant concentrations of wastewater-borne TiO₂NPs had a significant impact on the allocation time of *D. magna*. Therefore, this parameter should be

considered as a good behavioural marker for an effective assessment of the effects caused by TiO₂NPs.

4.6. Biochemical effects of wastewater-borne and ASTM-dispersed NPs

At the biochemical level, the negative impacts were generally more observed in *D. magna* exposed to wastewater-borne NPs compared with those animals exposed to ASTM-dispersed NPs. This was particularly evident for wastewater-borne AgNPs. These differences can be interpreted as a particular response of *D. magna* to the tested treatments. The wastewater-borne NPs probably induced the formation of reactive oxygen species (ROS) that enhanced particular toxicity mechanisms (Li et al., 2018; Liu and Wang, 2017). Furthermore, the likely formation of a DOM-protein eco-corona coating around wastewater-borne TiO₂NPs might have contributed to the limited irradiation of particle surfaces in the effluent, thus contributing to the potential scavenging of harmful ROS (Seitz et al., 2015; Shakiba et al., 2018). Regardless of the exposure matrices, the less significant effects of TiO₂NPs compared to AgNPs on the generality of the studied biochemical markers might have been due to the capability of the former to form stable agglomerates, thus becoming less available to animals (Sharma, 2009; Zhou et al., 2015).

4.6.1. Effects on AChE activity

In our study, there was an inhibition of AChE activity with 75 µg L⁻¹ of wastewater-borne AgNPs and with 12.5-25 µg L⁻¹ of ASTM-dispersed TiO₂NPs, thus suggesting neurotoxicity of both types of NPs, but not in a dose-dependent way. The available literature on the effects of metals, metal oxides and respective nano-counterparts on AChE activity revealed contradictory information due to the absence of standardization in experimental protocols, such as e.g. different species, exposure routes, dosing, sizes, and crystal forms of NPs (Šinko et al., 2014; Ulm et al., 2015). For example, our results are contrary to Ulm et al. (2015), which showed a concentration-dependent induction of AChE activity in *D. magna* neonates with 1-10 µg L⁻¹ of citrate-coated AgNPs (18.2 ± 10.1 nm) for 48 h. Yet, our findings are concordant with Katuli et al. (2014), who observed an inhibition of AChE activity in *D. rerio* erythrocytes with 2 and 4 mg L⁻¹ of AgNPs (25-100 nm) after 21 d. Furthermore, Khalil (2015) observed that 10, 50 and 100 µg kg⁻¹ of TiO₂NPs (anatase-rutile; 20-40 nm) inhibited the AChE activity of

the earthworm *Pheretima hawayana*, in a concentration-dependent manner, after 28 d. Guan et al. (2018) reported that AChE activity was inhibited in the blood clam *Tegillarca granosa* exposed to 0.1-10 mg L⁻¹ of TiO₂NPs (anatase; 35 ± 5 nm) for 96 h, thereby suggesting the occurrence of neurotoxicity associated mechanisms. Through *in vitro* assays, Wang et al. (2009) showed that the adsorption of 800 mg L⁻¹ of each rutile-DJ3 (50 nm) and anatase-HR3 (5-10 nm) TiO₂NPs to the AChE molecule inhibited its activity after 3 min. Although the inhibitory mechanism of AChE activity by AgNPs still remains unclear, it has been suggested that the long-term activity inhibition of human AChE is due to the released Ag⁺, which binds to the enzymatic complex and cause its irreversible inactivation through loss of protein structure caused by the reaction of Ag⁺ with the enzyme amino acids (Vrček and Šinko, 2013). This inhibitory response could also be explained by the adsorption of AChE onto the NP surface, with the subsequent inactivation of the enzyme due to conformational changes after surface coverage and ion release (Šinko et al., 2014; Vrček and Šinko, 2013; Wang et al., 2009). Furthermore, the significant induction of AChE activity with the highest concentration of wastewater-borne TiO₂NPs obtained in our study could be explained by a *de novo* synthesis of the enzyme to cope with the imposed stress. A similar compensatory mechanism was already reported in *D. magna* exposed to insecticides (Ren et al., 2017). Likewise, this adaptative mechanism was also observed in the marine scallop *Chlamys farreri* treated with 1 mg L⁻¹ of TiO₂NPs (anatase-rutile; 21 nm) for 14 d (Xia et al., 2017). Still, the detailed mechanism by which NPs inhibited or stimulated the AChE activity remains unclear in terms of the specific binding interactions between the enzyme and each particular type of NPs.

4.6.2. Effects on anaerobic metabolism

The evolution of LDH activity can function as a good biochemical marker of the anaerobic metabolism triggered by contaminants or other high-energy demanding factors. Although TiO₂NPs did not cause any effects on LDH activity of *D. magna*, overall there was an induction trend in its activity with wastewater-borne AgNPs, thus suggesting an increase of the anaerobic metabolism triggered by the imposed nanochemical stress.

4.6.3. Oxidative stress responses

In our study, it appears that ASTM-dispersed AgNPs did not cause any oxidative stress to *D. magna*. On the contrary, the wastewater-borne AgNPs seem to induce oxidative stress to the animals, since significant alterations in both GST and CAT activities were registered. Despite the inhibition of CAT activity at the lowest AgNP concentrations, the LPO levels were neither affected by wastewater-borne AgNPs nor by ASTM-dispersed AgNPs. In general, a similar response occurred in animals exposed to wastewater-borne TiO₂NPs and ASTM-dispersed TiO₂NPs. As pointed by Xiong et al. (2011), this might be explained by the low concentrations of both types of NPs, which were incapable of generating enough ROS to trigger oxidative lipid damage.

The inhibition of CAT activity with wastewater-borne AgNPs could be explained by the build-up of H₂O₂ and other ROS inside the cells, thus contributing to an imbalance between oxidative stress and the antioxidant defence system through a process of enzymatic denaturation, with a consequent loss of enzymatic activity. A similar inhibitory effect on CAT activity was obtained in the brain of two freshwater fish, viz. Nile tilapia (*Oreochromis niloticus*) and redbelly tilapia (*Tilapia zillii*) exposed to 4 mg L⁻¹ of AgNPs (< 100 nm), suggesting an over-accumulation of ROS which exceeded the scavenging ability of the antioxidant defence system, yet without any oxidative damage (Afifi et al., 2016). However, different results were obtained by Ulm et al. (2015), who observed an increase of CAT activity in *D. magna* neonates submitted for 48 h to 0.5-10 µg L⁻¹ of citrate-coated AgNPs (18.2 ± 10.1 nm) and 0.01-0.3 µg L⁻¹ of Ag⁺. These authors suggested that the induction of CAT activity with AgNPs are indicative of ROS production, while the induction and posterior decrease of its activity with increasing Ag⁺ concentrations was due to the increased production of hydroxyl radicals by Ag⁺, which led to a rapid inactivation of CAT activity caused by high H₂O₂ concentrations. As above-mentioned, the Ag⁺ is known to be released from AgNPs during oxidation processes, which requires both dissolved O₂ and H⁺, and this reaction culminates with the release of injurious peroxide intermediates, thereby leading to oxidative stress (Liu and Hurt, 2010).

Also relevant to our study was the induction of CAT activity with all tested concentrations of ASTM-dispersed TiO₂NPs, albeit only significant at the lowest one. These findings are substantiated by Klaper et al. (2009), which showed that the CAT activity of *Daphnia pulex* was enhanced by 75-500 mg L⁻¹ of TiO₂NPs (anatase, < 25 nm) after 24 h, thus reflecting oxidative stress. Canesi et al. (2010) showed that CAT and GST activities increased in the bivalve *Mytilus galloprovincialis* exposed to 1-5 mg L⁻¹ of TiO₂NPs (Evonik Aeroxide® P25; anatase-rutile; 21 nm) during 24 h. Nevertheless, in

our study, the GST activity was unchanged with ASTM-dispersed TiO₂NPs, which means that the imposed chemical stress was not strong enough to instigate other pathways involved in the antioxidant system after an apparent induction of CAT activity. Since the primary outcome of the antioxidant defence system after a cascade of reactions due to NP exposure is the activation of phase II detoxification enzymes, our results are in agreement with the hierarchical oxidative stress hypothesis initially proposed by Nel et al. (2006) which describes the three-tiered mechanism for NP-mediated oxidative stress.

5. CONCLUSIONS

The integrated approach, herein followed at both behavioural and biochemical level, clearly offered the advantage of allowing for an immediate (0 h) and early (96 h) detection of the health status of *D. magna* before the occurrence of more severe effects after longer exposure periods. Aligned with the published literature on the fate and effects of wastewater-borne NPs to aquatic biota, our findings went further in the state of the art and, for *D. magna* exposed to environmentally relevant concentrations of NPs, demonstrated that: (i) the wastewater-borne TiO₂NPs are prone to induce disturbances on *D. magna* swimming behaviour, particularly upon their prompt exposure; and (ii) even though wastewater-borne AgNPs caused minor effects on the swimming behaviour of the animals over 96 h, it is clear that their antioxidant machinery was affected by wastewater-borne AgNPs. In brief, the chosen behavioural-related parameters proved to be suitable for the assessment of toxic effects caused by wastewater-borne NPs in *D. magna*. Besides, the battery of selected biochemical markers can effectively function as important warning indicators for the detection of adverse effects caused by this type of xenobiotics. Accordingly, this behavioural-biochemical integrative approach can therefore provide essential and early warning background information to the environmental policymakers and stakeholders enrolled in the environmental risk assessment of NPs present in WWTP effluents.

Although the toxicological effects induced by wastewater-borne NPs may vary due to different factors, like *e.g.* type of NPs, exposure medium, dispersing agent, *etc.*, our findings added relevant information to the current topic. Regarding the way by which wastewater-borne NPs interact with biotic (*e.g.* molecules, cells, individuals) and/or abiotic (*e.g.* pH, ionic strength, DOM) variables within the effluent, it is likely that their mechanism of action could be much more complex compared to the corresponding one

after dispersion in less elaborate matrices, like *e.g.* ASTM medium. Besides NPs, the presence of additional substances and unknown xenobiotics in the effluent should also be considered in forthcoming investigations. Therefore, it will be advisable to gather additional data about the interaction of biotic and abiotic factors regarding each NP-matrix interaction in order to better comprehend the associated toxicological mechanisms. Also important is the choice of suitable dispersion agents during NP manufacturing, since some detrimental effects were observed with the chemicals used for AgNP solubilisation. This highlights the need for a deeper understanding of the chemical composition of the dispersion agent in order to better comprehend the potential resulting side-effects within a particular dispersion, not only in standardized laboratory media but also in more complex matrices. In this regard, the aggregation state of wastewater-borne NPs could inevitably change in complex environments and there is still a gap in the discussion about the use of suitable solubilizing agents in the view of their environmental relevance. Arguably, the use of natural compounds, like *e.g.* DOM would be of greater relevance since they occur in realistic scenarios. Bearing these environmental implications in mind, future integrated approaches should contemplate longer periods of time, like those followed in chronic and multi-generational studies. Concluding, the usual ecotoxicity tests carried out in the laboratory to evaluate NP toxicity from wastewater effluents should involve other than the routinely used synthetic waters as they may underestimate the toxicity of NPs.

Declaration of interests

The authors declare that they have no known competing financial interests or personal relationships that could have appeared to influence the work reported in this paper.

Acknowledgements:

This work was funded by the ERANET SIINN project FENOMENO (Fate and Effect of Wastewater-borne Manufactured Nanomaterials in Aquatic Ecosystems; Grant No.: 03XP0005). Thanks are due for the financial support to CESAM (UID/AMB/50017/2019), to FCT/MEC through national funds, and to the co-funding by the FEDER, within the PT2020 Partnership Agreement and Compete 2020. The work of VG and MSM is funded by national funds (OE), through FCT – Fundação para a Ciência e a Tecnologia, I.P., in the scope of the framework contract foreseen in the numbers 4, 5

and 6 of the Article 23, of the Decree-Law 57/2016, of August 29, changed by Law 57/2017, of July 19. Further funding by the Federal Ministry of Education and Research (BMBF; 03XP0005A), Fraunhofer IME and the University of Siegen are also gratefully acknowledged. Part of this work was performed at the Micro- and Nanoanalytics Facility (MNaF) at the University of Siegen.

Journal Pre-proof

References

Adam, V., Caballero-Guzman, A., Nowack, B., 2018. Considering the forms of released engineered nanomaterials in probabilistic material flow analysis. *Environ Pollut* 243, 17-27.

Afifi, M., Saddick, S., Abu Zinada, O.A., 2016. Toxicity of silver nanoparticles on the brain of *Oreochromis niloticus* and *Tilapia zillii*. *Saudi J. Biol. Sci.* 23, 754-760.

Bownik, A., 2017. *Daphnia* swimming behaviour as a biomarker in toxicity assessment: a review. *Sci. Total Environ.* 601, 194-205.

Bradford, M.M., 1976. A rapid and sensitive method for quantitation of microgram quantities of protein utilizing principle of protein-dye binding. *Anal. Biochem.* 72, 248-254.

Brar, S.K., Verma, M., Tyagi, R.D., Surampalli, R.Y., 2010. Engineered nanoparticles in wastewater and wastewater sludge - Evidence and impacts. *Waste Manage* 30, 504-520.

Breheny, P., Burchett, W., 2016. Package 'visreg': Visualization of Regression Models. Ver. 2.5-0. R-Project [Online]. Available: <https://cran.r-project.org/web/packages/visreg/visreg.pdf> (last updated: 2018/02/26; last accessed: 2020/01/03).

Canesi, L., Fabbri, R., Gallo, G., Vallotto, D., Marcomini, A., Pojana, G., 2010. Biomarkers in *Mytilus galloprovincialis* exposed to suspensions of selected nanoparticles (Nano carbon black, C60 fullerene, Nano-TiO₂, Nano-SiO₂). *Aquat. Toxicol.* 100, 168-177.

Clairborne, A., 1985. Catalase activity, in: Greenwald, R.A. (Ed.), *CRC Handbook of Methods for Oxygen Radical Research*. CRC Press, Boca Ration, FL, pp. 283-284.

Coll, C., Notter, D., Gottschalk, F., Sun, T., Som, C., Nowack, B., 2016. Probabilistic environmental risk assessment of five nanomaterials (nano-TiO₂, nano-Ag, nano-ZnO, CNT, and fullerenes). *Nanotoxicology* 10, 436-444.

Čolović, M.B., Krstić, D.Z., Lazarević-Pašti, T.D., Bondžić, A.M., Vasić, V.M., 2013. Acetylcholinesterase inhibitors: pharmacology and toxicology. *Curr. Neuropharmacol.* 11, 315-335.

Cupi, D., Hartmann, N.B., Baun, A., 2015. The influence of natural organic matter and aging on suspension stability in guideline toxicity testing of silver, zinc oxide, and

titanium dioxide nanoparticles with *Daphnia magna*. Environ. Toxicol. Chem. 34, 497-506.

Dabrunz, A., Duester, L., Prasse, C., Seitz, F., Rosenfeldt, R., Schilde, C., Schaumann, G.E., Schulz, R., 2011. Biological surface coating and molting inhibition as mechanisms of TiO₂ nanoparticle toxicity in *Daphnia magna*. PLoS One 6, e20112.

Deng, R., Lin, D., Zhu, L., Majumdar, S., White, J.C., Gardea-Torresdey, J.L., Xing, B., 2017. Nanoparticle interactions with co-existing contaminants: joint toxicity, bioaccumulation and risk. Nanotoxicology 11, 591-612.

Diamantino, T.C., Almeida, E., Soares, A.M.V.M., Guilhermino, L., 2001. Lactate dehydrogenase activity as an effect criterion in toxicity tests with *Daphnia magna* straus. Chemosphere 45, 553-560.

Ellman, G.L., Courtney, K.D., Andres Jr., V., Featherstone, R.M., 1961. A new and rapid colorimetric determination of acetylcholinesterase activity. Biochem. Pharmacol. 7, 88-95.

Franze, B., Strenge, I., Engelhard, C., 2017. Separation and detection of gold nanoparticles with capillary electrophoresis and ICP-MS in single particle mode (CE-SP-ICP-MS). J Anal Atom Spectrom 32, 1481-1489.

Gartiser, S., Flach, F., Nickel, C., Stintz, M., Damme, S., Schaeffer, A., Erdinger, L., Kuhlbusch, T.A.J., 2014. Behavior of nanoscale titanium dioxide in laboratory wastewater treatment plants according to OECD 303 A. Chemosphere 104, 197-204.

Georgantzopoulou, A., Carvalho, P.A., Vogelsang, C., Tilahun, M., Ndungu, K., Booth, A.M., Thomas, K.V., Macken, A., 2018. Ecotoxicological effects of transformed silver and titanium dioxide nanoparticles in the effluent from a lab-scale wastewater treatment system. Environ. Sci. Technol. 52, 9431-9441.

Guan, X., Shi, W., Zha, S., Rong, J., Su, W., Liu, G., 2018. Neurotoxic impact of acute TiO₂ nanoparticle exposure on a benthic marine bivalve mollusk, *Tegillarca granosa*. Aquat. Toxicol. 200, 241-246.

Guilhermino, L., Lopes, M.C., Carvalho, A.P., Soares, A.M.V.M., 1996. Inhibition of acetylcholinesterase activity as effect criterion in acute tests with juvenile *Daphnia magna*. Chemosphere 32, 727-738.

Habig, W.H., Pabst, M.J., Jakoby, W.B., 1974. Glutathione S-transferases - The first enzymatic step in mercapturic acid formation. J. Biol. Chem. 249, 7130-7139.

Handy, R.D., Cornelis, G., Fernandes, T., Tsyusko, O., Decho, A., Sabo-Attwood, T., Metcalfe, C., Steevens, J.A., Klaine, S.J., Koelmans, A.A., Horne, N., 2012.

Ecotoxicity test methods for engineered nanomaterials: practical experiences and recommendations from the bench. *Environ. Toxicol. Chem.* 31, 15-31.

Hartmann, G., Hutterer, C., Schuster, M., 2013. Ultra-trace determination of silver nanoparticles in water samples using cloud point extraction and ETAAS. *J. Anal. Atom. Spectrom.* 28, 567-572.

Hartmann, S., Louch, R., Zeumer, R., Steinhoff, B., Mozhayeva, D., Engelhard, C., Schönherr, H., Schlechtriem, D., Witte, K., 2019. Comparative multi-generation study on long-term effects of pristine and wastewater-borne silver and titanium dioxide nanoparticles on key lifecycle parameters in *Daphnia magna*. *NanoImpact* 14, 100163. DOI: <https://doi.org/10.1016/j.impact.2019.100163>.

Jacobasch, C., Volker, C., Giebner, S., Volker, J., Alsenz, H., Potouridis, T., Heidenreich, H., Kayser, G., Oehlmann, J., Oetken, M., 2014. Long-term effects of nanoscaled titanium dioxide on the cladoceran *Daphnia magna* over six generations. *Environ Pollut* 186, 180-186.

Justice, J.R., Bernot, R.J., 2014. Nanosilver inhibits freshwater gastropod (*Physa acuta*) ability to assess predation risk. *Am. Midl. Nat.* 171, 340-349.

Kaegi, R., Voegelin, A., Sinnet, B., Zuleeg, S., Hagendorfer, H., Burkhardt, M., Siegrist, H., 2011. Behavior of metallic silver nanoparticles in a pilot wastewater treatment plant. *Environ. Sci. Technol.* 45, 3902-3908.

Kahru, A., Ivask, A., 2013. Mapping the dawn of nanoecotoxicological research. *Acc. Chem. Res.* 46, 823-833.

Katuli, K.K., Massarsky, A., Hadadi, A., Pourmehran, Z., 2014. Silver nanoparticles inhibit the gill Na^+/K^+ -ATPase and erythrocyte AChE activities and induce the stress response in adult zebrafish (*Danio rerio*). *Ecotox. Environ. Safe.* 106, 173-180.

Khalil, A.M., 2015. Neurotoxicity and biochemical responses in the earthworm *Pheretima hawayana* exposed to TiO_2 NPs. *Ecotox. Environ. Safe.* 122, 455-461.

Kim, Y., Farnazo, D.M., 2017. Toxicity characteristics of sewage treatment effluents and potential contribution of micropollutant residuals. *J. Ecol. Environ.* 41, 10 pp.

Kiser, M.A., Westerhoff, P., Benn, T., Wang, Y., Pérez-Rivera, J., Hristovski, K., 2009. Titanium nanomaterial removal and release from wastewater treatment plants. *Environ. Sci. Technol.* 43, 6757-6763.

Klaper, R., Crago, J., Barr, J., Arndt, D., Setyowati, K., Chen, J., 2009. Toxicity biomarker expression in daphnids exposed to manufactured nanoparticles: changes in toxicity with functionalization. *Environ Pollut* 157, 1152-1156.

Kühr, S., Schneider, S., Meisterjahn, B., Schlich, K., Hund-Rinke, K., Schlechtriem, C., 2018. Silver nanoparticles in sewage treatment plant effluents: chronic effects and accumulation of silver in the freshwater amphipod *Hyaella azteca*. *Environ. Sci. Eur.* 30, 11.

Kunze, J., Hartmann, S., Witte, K., Kuhnert, J.-D., 2016. *Daphnia magna* as biosensor for Ag-nanoparticles in water systems: development of a computer vision system for the detection of behavioral changes. In: *Book of Abstracts of the ICPR 2016 - 23rd International Conference on Pattern Recognition (Dez. 4-6, 2016)*. Workshop on Visual Observation and Analysis of Animal and Insect Behavior (VAIB). Cancún, Mexico.

Kuznetsova, A., Brockhoff, P.B., Christensen, R.H.B., 2017. lmerTest package: tests in linear mixed effects models. *J. Stat. Softw.*, 82(13). DOI: <https://doi.org/10.18637/jss.v082.i13>.

Lai, R.W.S., Yeung, K.W.Y., Yung, M.M.N., Djurišić, A.B., Giesy, J.P., Leung, K.M.Y., 2018. Regulation of engineered nanomaterials: current challenges, insights and future directions. *Environ. Sci. Pollut. Res.* 25, 3060-3077.

Lazareva, A., Keller, A.A., 2014. Estimating potential life cycle releases of engineered nanomaterials from wastewater treatment plants. *ACS Sustain. Chem. Eng.* 2, 1656-1665.

Li, Y., Zhao, J., Shang, E., Xia, X., Niu, J., Crittenden, J., 2018. Effects of chloride ions on dissolution, ROS generation, and toxicity of silver nanoparticles under UV irradiation. *Environ. Sci. Technol.* 52, 4842-4849.

Liu, J., Hurt, R.H., 2010. Ion release kinetics and particle persistence in aqueous nano-silver colloids. *Environ. Sci. Technol.* 44, 2169-2175.

Liu, J., Wang, W.-X., 2017. The protective roles of TiO₂ nanoparticles against UV-B toxicity in *Daphnia magna*. *Sci. Total Environ.* 593, 47-53.

Lovern, S.B., Klaper, R., 2006. *Daphnia magna* mortality when exposed to titanium dioxide and fullerene (C₆₀) nanoparticles. *Environ. Toxicol. Chem.* 25, 1132-1137.

Mahlalela, L.C., Ngila, J.C., Dlamini, L.N., 2017. Monitoring the fate and behavior of TiO₂ nanoparticles: simulated in a WWTP with industrial dye-stuff effluent

according to OECD 303A. J. Environ. Sci. Health Part A-Toxic/Hazard. Subst. Environ. Eng. 52, 794-803.

Maurer-Jones, M.A., Gunsolus, I.L., Murphy, C.J., Haynes, C.L., 2013. Toxicity of engineered nanoparticles in the environment. Anal Chem 85, 3036-3049.

Mozhayeva, D., Engelhard, C., 2017. Separation of silver nanoparticles with different coatings by capillary electrophoresis coupled to ICP-MS in single particle mode. Anal. Chem. 89, 9767-9774.

Mozhayeva, D., Engelhard, C., 2019. A quantitative nanoparticle extraction method for microsecond time resolved single-particle ICP-MS data in the presence of high background. J. Anal. At. Spectrom. 34, 1571-1580.

Mozhayeva, D., Engelhard, C., 2020. A critical review of single particle inductively coupled plasma mass spectrometry - A step towards an ideal method for nanomaterial characterization. J. Anal. At. Spectrom, DOI: 10.1039/c9ja00206e.

Mozhayeva, D., Strenge, I., Engelhard, C., 2017. Implementation of online preconcentration and microsecond time resolution to capillary electrophoresis single particle inductively coupled plasma mass spectrometry (CE-SP-ICP-MS) and its application in silver nanoparticle analysis. Anal. Chem. 89, 7152-7159.

Muth-Köhne, E., Sonnack, L., Schlich, K., Hischen, F., Baumgartner, W., Hund-Rinke, K., Schäfers, C., Fenske, M., 2013. The toxicity of silver nanoparticles to zebrafish embryos increases through sewage treatment processes. Ecotoxicology 22, 1264-1277.

Nel, A., Xia, T., Mädler, L., Li, N., 2006. Toxic potential of materials at the nanolevel. Science 311, 622-627.

Noss, C., Dabrunz, A., Rosenfeldt, R.R., Lorke, A., Schulz, R., 2013. Three-dimensional analysis of the swimming behavior of *Daphnia magna* exposed to nanosized titanium dioxide. PLoS One 8, e80960.

OECD, 2001. *OECD Guideline for the Testing of Chemicals. Test No. 303: Simulation Test - Aerobic Sewage Treatment (303A: Activated Sludge Units; 303B: Biofilms)*. OECD Publishing, Paris, France.

OECD, 2004. *OECD Guideline for the Testing of Chemicals. Test No. 202: Daphnia sp., Acute Immobilisation Test*. OECD Publishing, Paris, France.

OECD, 2016. *Nanomaterials in Waste Streams: Current Knowledge on Risks and Impacts*. OECD Publishing, Paris.

Ohkawa, H., Ohishi, N., Yagi, K., 1979. Assay for lipid peroxides in animal tissues by thiobarbituric acid reaction. Anal. Biochem. 95, 351-358.

Pettersson, A., Adamsson, M., Dave, G., 2000. Toxicity and detoxification of Swedish detergents and softener products. *Chemosphere* 41, 1611-1620.

Pokhrel, L.R., Dubey, B., 2012. Potential impact of low-concentration silver nanoparticles on predator-prey interactions between predatory dragonfly nymphs and *Daphnia magna* as a prey. *Environ. Sci. Technol.* 46, 7755-7762.

Poynton, H.C., Lazorchak, J.M., Impellitteri, C.A., Blalock, B.J., Rogers, K., Allen, H.J., Loguinov, A., Heckrnan, J.L., Govindasmawy, S., 2012. Toxicogenomic responses of nanotoxicity in *Daphnia magna* exposed to silver nitrate and coated silver nanoparticles. *Environ. Sci. Technol.* 46, 6288-6296.

Ratte, H.T., 1999. Bioaccumulation and toxicity of silver compounds: a review. *Environ. Toxicol. Chem.* 18, 89-108.

Ren, M., Horn, H., Frimmel, F.H., 2017. Aggregation behavior of TiO₂ nanoparticles in municipal effluent: influence of ionic strength and organic compounds. *Water Res.* 123, 678-686.

Ribeiro, F., Van Gestel, C.A.M., Pavlaki, M.D., Azevedo, S., Soares, A.M.V.M., Loureiro, S., 2017. Bioaccumulation of silver in *Daphnia magna*: waterborne and dietary exposure to nanoparticles and dissolved silver. *Sci. Total Environ.* 574, 1633-1639.

Ritz, C., Strebig, J.C., Ritz, C., 2016. Package 'drc': Analysis of Dose-Response Curves. Ver. 3.0-1. R-Project [Online]. Available: <https://cran.r-project.org/web/packages/drc/drc.pdf> (last updated: 2016/08/25; last accessed on 2020/01/03).

Roco, M.C., Mirkin, C.A., Hersam, M.C., 2011. Nanotechnology Research Directions for Societal Needs in 2020: Retrospective and Outlook. Springer, Dordrecht, The Netherlands.

Seitz, F., Lüderwald, S., Rosenfeldt, R.R., Schulz, R., Bundschuh, M., 2015. Aging of TiO₂ nanoparticles transiently increases their toxicity to the pelagic microcrustacean *Daphnia magna*. *PLoS One* 10, e0126021.

Shakiba, S., Hakimian, A., Barco, L.R., Louie, S.M., 2018. Dynamic intermolecular interactions control adsorption from mixtures of natural organic matter and protein onto titanium dioxide nanoparticles. *Environ. Sci. Technol.* 52, 14158-14168.

Sharma, V.K., 2009. Aggregation and toxicity of titanium dioxide nanoparticles in aquatic environment-A review. *J. Environ. Sci. Health Part A-Toxic/Hazard. Subst. Environ. Eng.* 44, 1485-1495.

Šinko, G., Vrček, I.V., Goessler, W., Leitinger, G., Dijanošić, A., Miljanić, S., 2014. Alteration of cholinesterase activity as possible mechanism of silver nanoparticle toxicity. *Environ. Sci. Pollut. Res.* 21, 1391-1400.

Streng, I., Engelhard, C., 2016. Capabilities of fast data acquisition with microsecond time resolution in inductively coupled plasma mass spectrometry and identification of signal artifacts from millisecond dwell times during detection of single gold nanoparticles. *J Anal Atom Spectrom* 31, 135-144.

Sun, T.Y., Gottschalk, F., Hungerbühler, K., Nowack, B., 2014. Comprehensive probabilistic modelling of environmental emissions of engineered nanomaterials. *Environ Pollut* 185, 69-76.

Svanström, M., Bertanza, G., Bolzonella, D., Canato, M., Collivignarelli, C., Heimersson, S., Laera, G., Mininni, G., Peters, G., Tomei, M.C., 2014. Method for technical, economic and environmental assessment of advanced sludge processing routes. *Water Sci Technol* 69, 2407-2416.

Szulkin, M., Dawidowicz, P., Dodson, S.I., 2006. Behavioural uniformity as a response to cues of predation risk. *Anim. Behav.* 71, 1013-1019.

Ulm, L., Krivohlavek, A., Jurašin, D., Ljubojević, M., Šinko, G., Crnković, T., Žuntar, I., Šikić, S., Vrček, I.V., 2015. Response of biochemical biomarkers in the aquatic crustacean *Daphnia magna* exposed to silver nanoparticles. *Environ. Sci. Pollut. Res.* 22, 19990-19999.

Uttieri, M., Mazzocchi, M.G., Ai, N., D'Alcalà, M.R., Strickler, J.R., Zambianchi, E., 2004. Lagrangian description of zooplankton swimming trajectories. *J. Plankton Res.* 26, 99-105.

Uttieri, M., Zambianchi, E., Strickler, J.R., Mazzocchi, M.G., 2005. Fractal characterization of three-dimensional zooplankton swimming trajectories. *Ecol. Model.* 185, 51-63.

Vassault, A., 1983. Lactate dehydrogenase: UV-method with pyruvate and NADH, in: Bergmeyer, H.-U. (Ed.), *Methods of Enzymatic Analysis, Volume 3 - Enzymes 1: Oxidoreductases, Transferases*. Academic Press, Inc., New York, pp. 118-126.

Völker, C., Boedicker, C., Daubenthaler, J., Oetken, M., Oehlmann, J., 2013a. Comparative toxicity assessment of nanosilver on three *Daphnia* species in acute, chronic and multi-generation experiments. *PLoS One* 8, e75026.

Völker, C., Oetken, M., Oehlmann, J., 2013b. The biological effects and possible modes of action of nanosilver. *Rev. Environ. Contam. Toxicol.* 223, 81-106.

Vrček, I.V., Šinko, G., 2013. Inactivation of cholinesterases by silver and gold ions *in vitro*. *Cent. Eur. J. Chem.* 11, 935-944.

Wang, Z., Zhao, J., Li, F., Gao, D., Xing, B., 2009. Adsorption and inhibition of acetylcholinesterase by different nanoparticles. *Chemosphere* 77, 67-73.

Wu, J., Zhu, G., Yu, R., 2018. Fates and impacts of nanomaterial contaminants in biological wastewater treatment system: a review. *Water Air Soil Pollut.* 229, 21.

Xia, B., Zhu, L., Han, Q., Sun, X., Chen, B., Qu, K., 2017. Effects of TiO₂ nanoparticles at predicted environmental relevant concentration on the marine scallop *Chlamys farreri*: an integrated biomarker approach. *Environ. Toxicol. Pharmacol.* 50, 128-135.

Xiong, D., Fang, T., Yu, L., Sima, X., Zhu, W., 2011. Effects of nano-scale TiO₂, ZnO and their bulk counterparts on zebrafish: acute toxicity, oxidative stress and oxidative damage. *Sci. Total Environ.* 409, 1444-1452.

Zhang, Y., Qiang, L., Yuan, Y., Wu, W., Sun, B., Zhu, L., 2018. Impacts of titanium dioxide nanoparticles on transformation of silver nanoparticles in aquatic environments. *Environ.-Sci. Nano* 5, 1191-1199.

Zhou, X.-h., Huang, B.-c., Zhou, T., Liu, Y.-c., Shi, H.-c., 2015. Aggregation behavior of engineered nanoparticles and their impact on activated sludge in wastewater treatment. *Chemosphere* 119, 568-576.

Figure captions:

Fig. 1. High-angle annular dark-field scanning transmission electron microscopy images and elemental maps of (A) wastewater-borne AgNPs and (B) ASTM-dispersed AgNPs. The energy-dispersive x-ray spectra correspond to the highlighted regions of interest.

Fig. 2. High-angle annular dark-field scanning transmission electron microscopy images and elemental maps of (A) wastewater-borne TiO₂NPs and (B) ASTM-dispersed TiO₂NPs. The energy-dispersive x-ray spectra correspond to the highlighted regions of interest.

Fig. 3. Mean particle size \pm SE of the Gaussian distribution of (A) AgNPs and (B) TiO₂NPs dispersed in ASTM medium at the tested concentrations, and monitored over 96 h. Results of single particle inductively coupled plasma mass spectroscopy with 5 μ s time resolution.

Fig. 4. Swimming height (mean \pm SE) of *Daphnia magna* (N = 4-5; 9-10 animals per replicate) exposed to wastewater-borne and ASTM-dispersed AgNPs at 0 and 96 h. Effluent (EFF), dispersing agent (DA) and negative control (CT) are the experimental controls. The • indicates significant differences between NP concentrations dispersed in the same media at different time points (two-way ANOVA followed by Tukey's *post-hoc* test; $p < 0.05$).

Fig. 5. Swimming height (mean \pm SE) of *Daphnia magna* (N = 5; 9-10 animals per replicate) exposed to wastewater-borne and ASTM-dispersed TiO₂NPs at 0 and 96 h. Effluent (EFF) and negative control (CT) are the experimental controls. The * denotes significant differences of each NP concentration compared to the respective control; • indicates significant differences between identical controls or identical NP concentrations dispersed in the same media at different time points; # represents significant differences between identical NP concentrations tested in different exposure media at a particular time point (two-way ANOVA followed by Tukey's *post-hoc* test; $p < 0.05$).

Fig. 6. Conditional plots for the allocation time of *Daphnia magna* exposed to different AgNP treatments (test media + NPs) at 0 and 96 h for each zone of the vessel (1, top; 2, central, or 3, bottom), predicted for controls (0 h: **A, C**; 96 h: **B, D**) and concentration gradient of AgNPs (0 h: **E, G**; 96 h: **F, H**). Each panel illustrates the effects at 0 and 96 h, respectively, between: (**A, B**) dispersing agent (DA) and negative (CT) controls; (**C, D**) effluent (EFF) and negative (CT) controls; and different concentrations of (**E, F**) wastewater-borne AgNPs and (**G, H**) ASTM-dispersed AgNPs. Dots represent partial residuals; lines with shaded zones are regression lines and respective confidence intervals.

Fig. 7. Conditional plots for the allocation time of *Daphnia magna* exposed to different TiO₂NP treatments (test media + NPs) at 0 and 96 h for each zone of the vessel (1, top; 2, central, or 3, bottom), predicted for controls (0 h: **A**; 96 h: **B**) and concentration gradient of TiO₂NPs (0 h: **C, E**; 96 h: **D, F**). Each panel illustrates the effects at 0 and 96 h, respectively, between: (**A, B**) effluent (EFF) and negative (CT) controls; and different concentrations of (**C, D**) wastewater-borne TiO₂NPs and (**E, F**) ASTM-dispersed TiO₂NPs. Dots represent partial residuals; lines with shaded zones are regression lines and respective confidence intervals.

Fig. 8. Enzymatic activities (mean \pm SE) of (**A, B**) acetylcholinesterase (AChE), (**C, D**) lactate dehydrogenase (LDH), (**E, F**) glutathione *S*-transferase, (**G, H**) catalase, and (**I, J**) lipid peroxidation (LPO) levels of *Daphnia magna* (N = 3-4; 9-10 animals per replicate) after a 96 h exposure to AgNPs (**A, C, E, G, I**) and TiO₂NPs (**B, D, F, H, J**), presented as wastewater-borne and dispersed in ASTM medium. Effluent (EFF), ASTM medium (CT) and dispersing agent (DA) are NP-free controls. The * represents significant differences relatively to controls (t-test or one-way ANOVA followed by Dunnett's *post-hoc* test); # represents significant differences (t-test) between identical NP concentrations or between different controls within different media ($p < 0.05$).

Fig. 1.

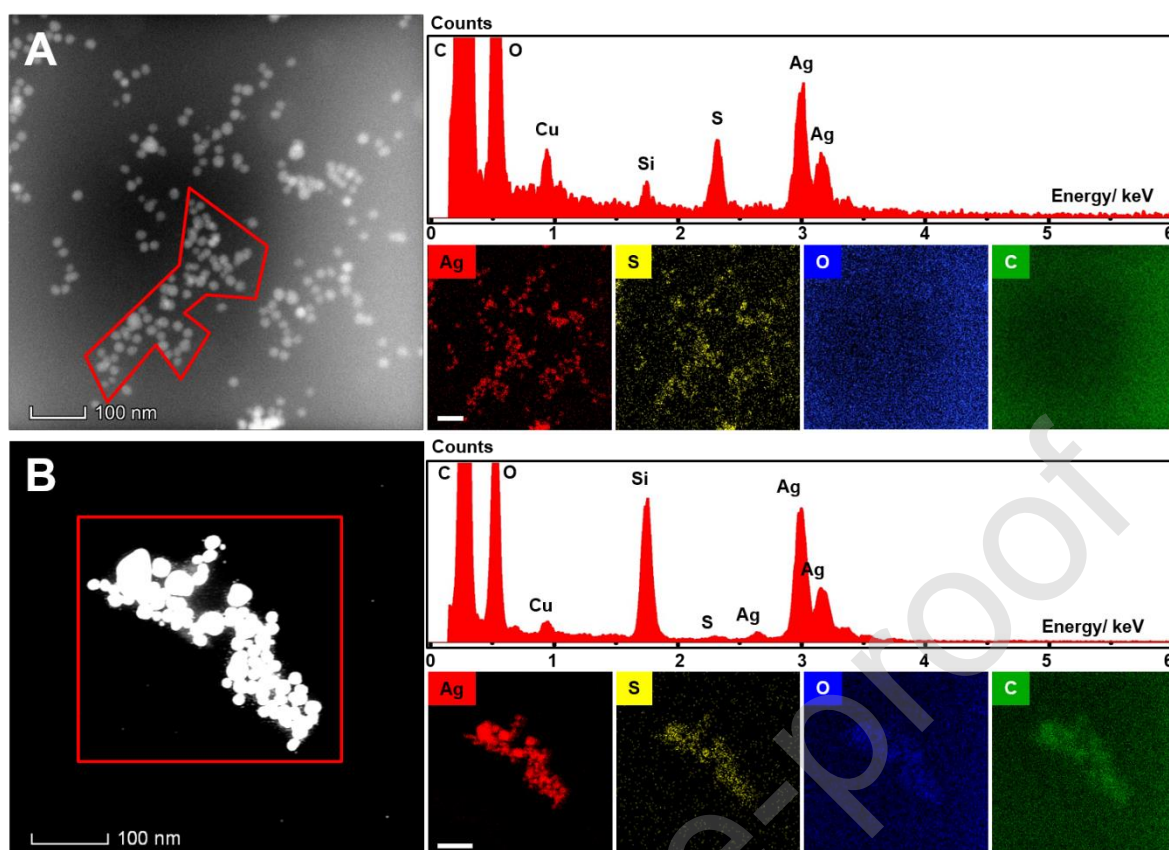


Fig. 2.

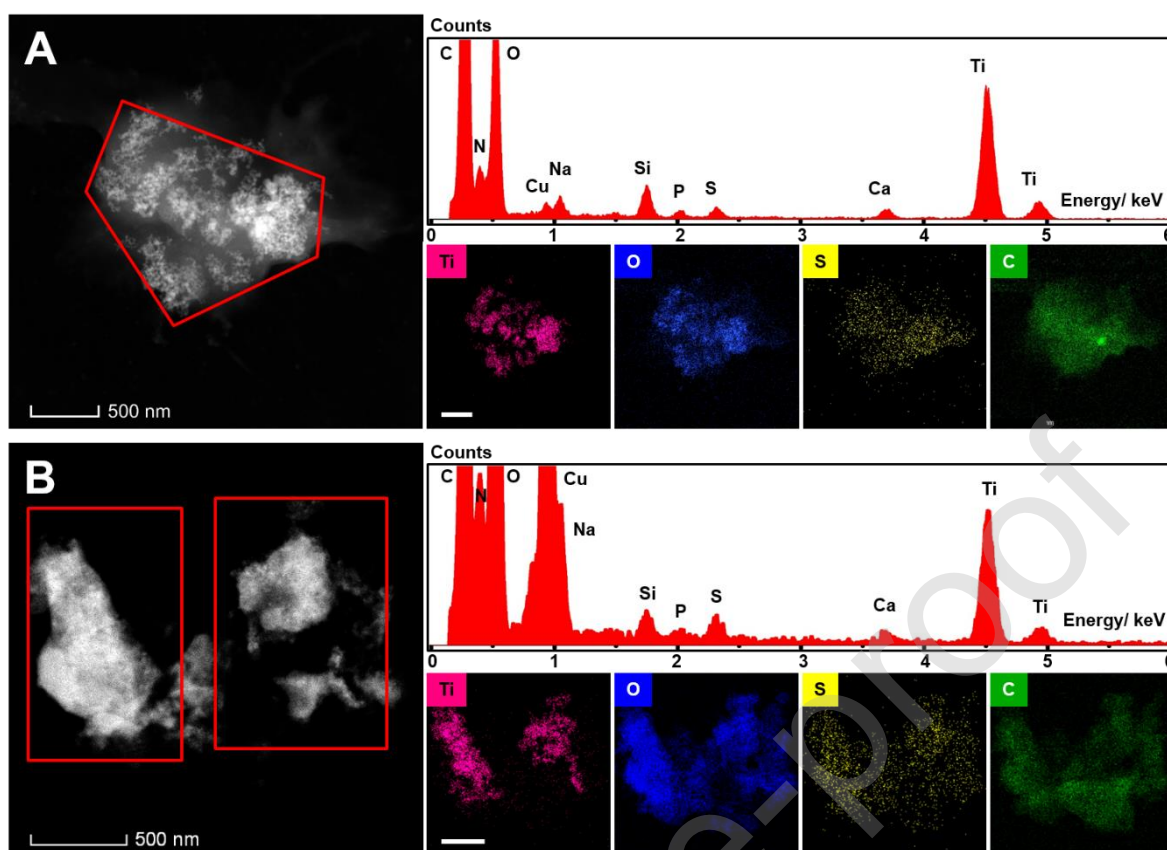


Fig. 3.

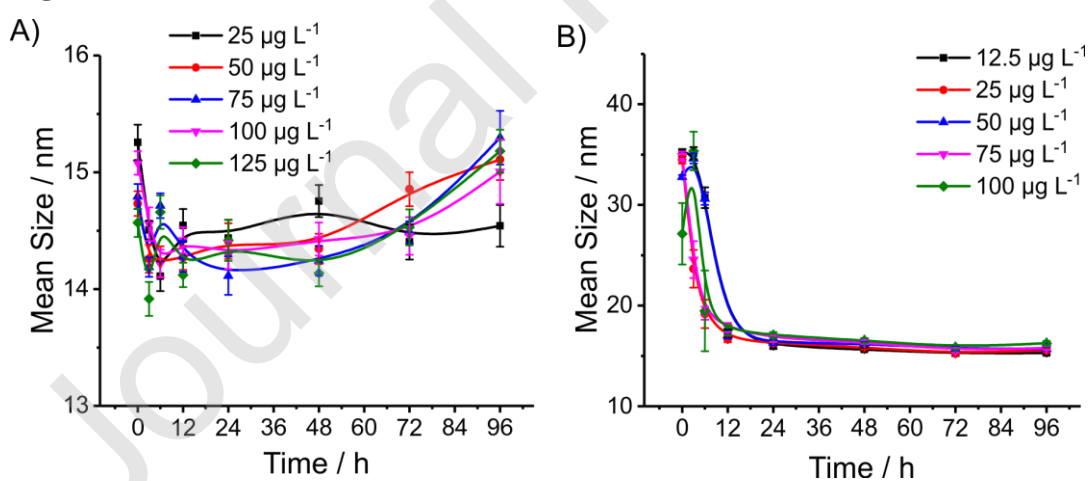


Fig. 4.

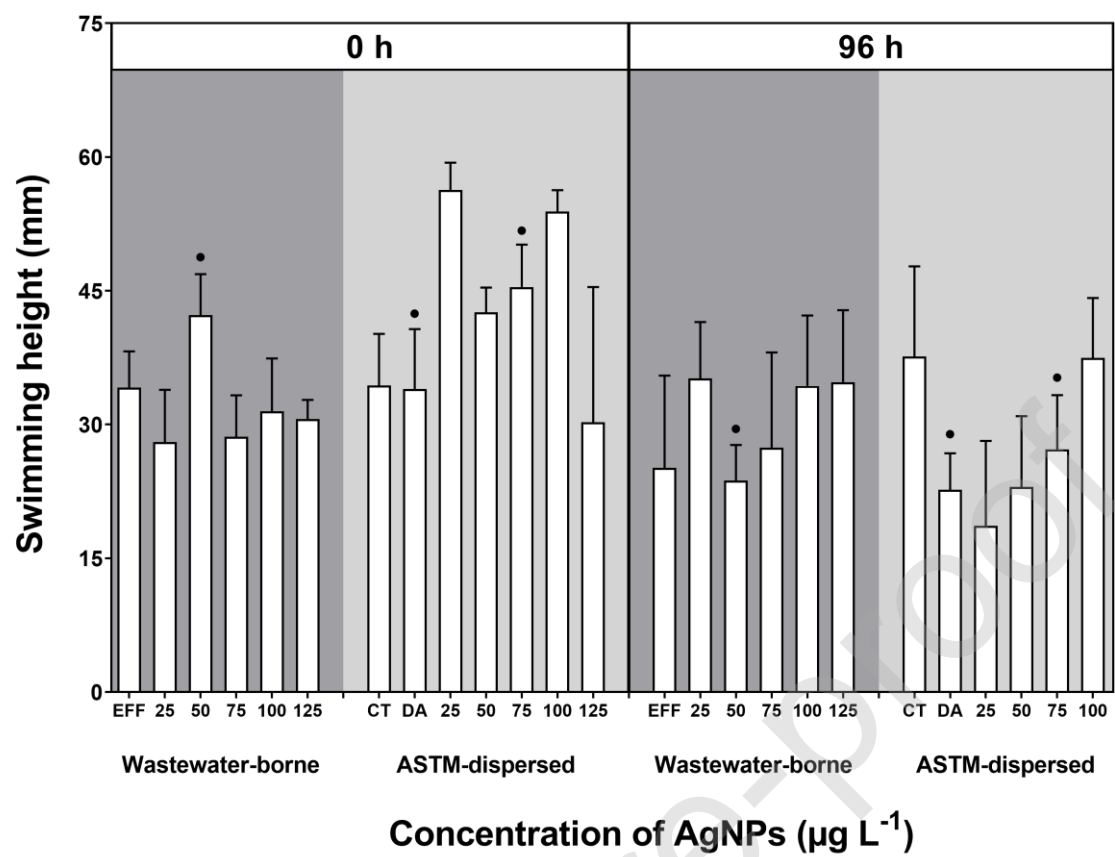


Fig. 5.

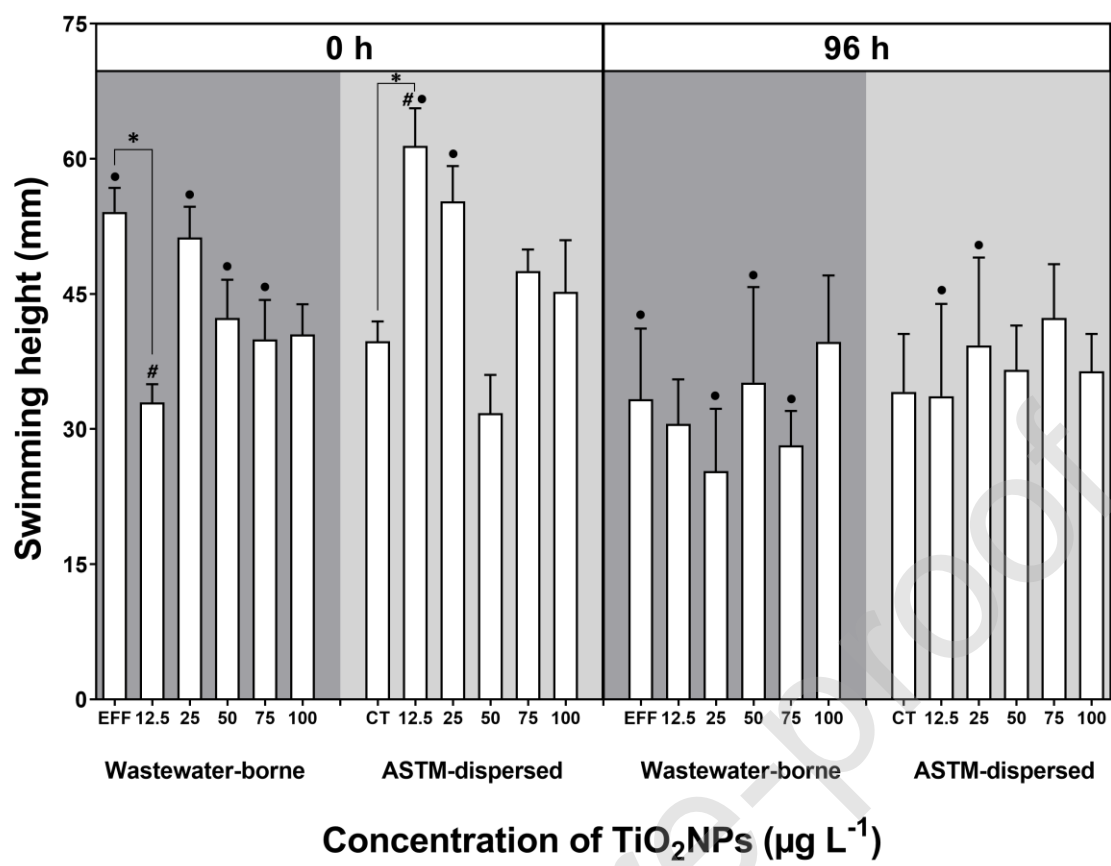


Fig. 6.

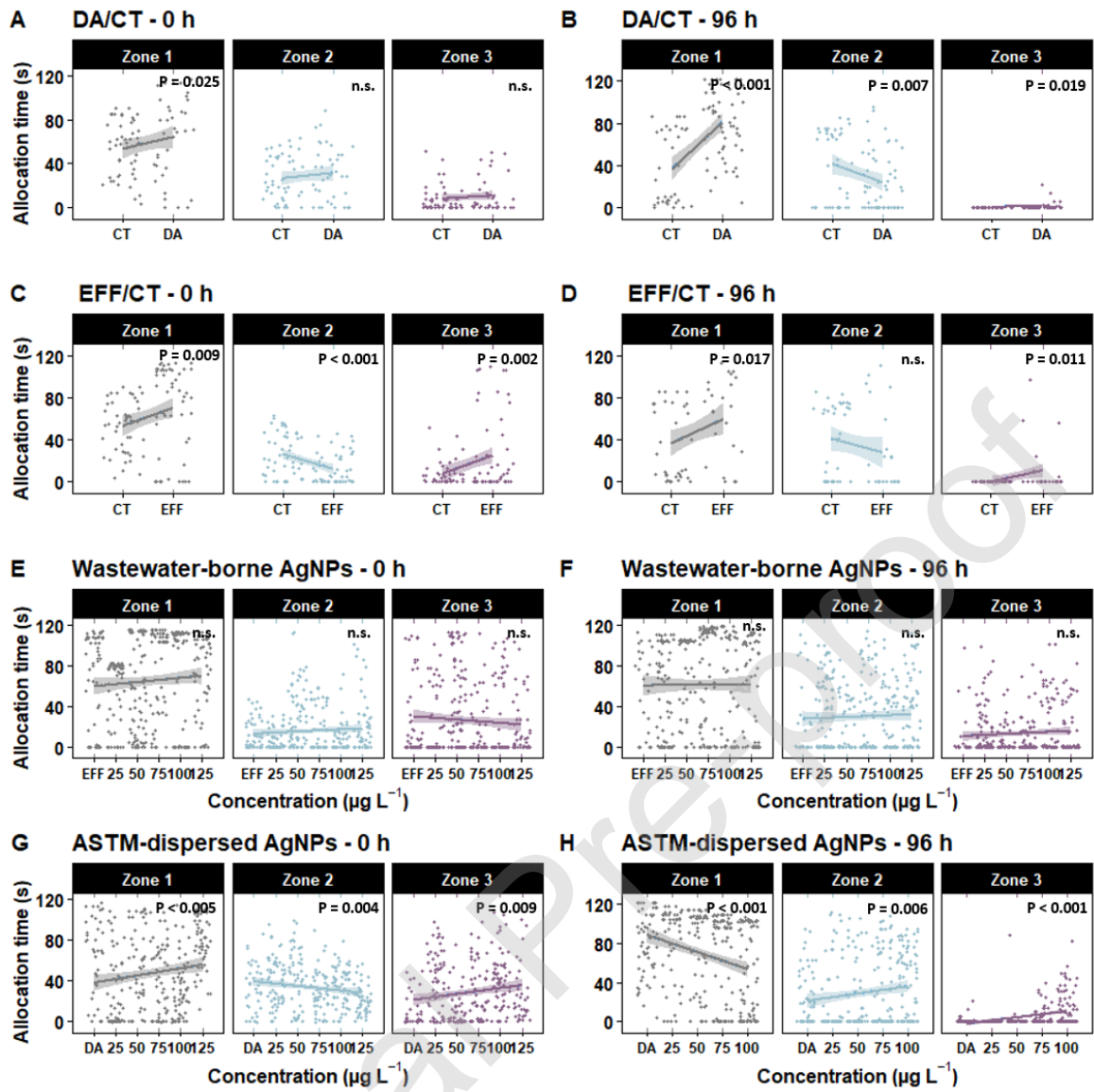


Fig. 7.

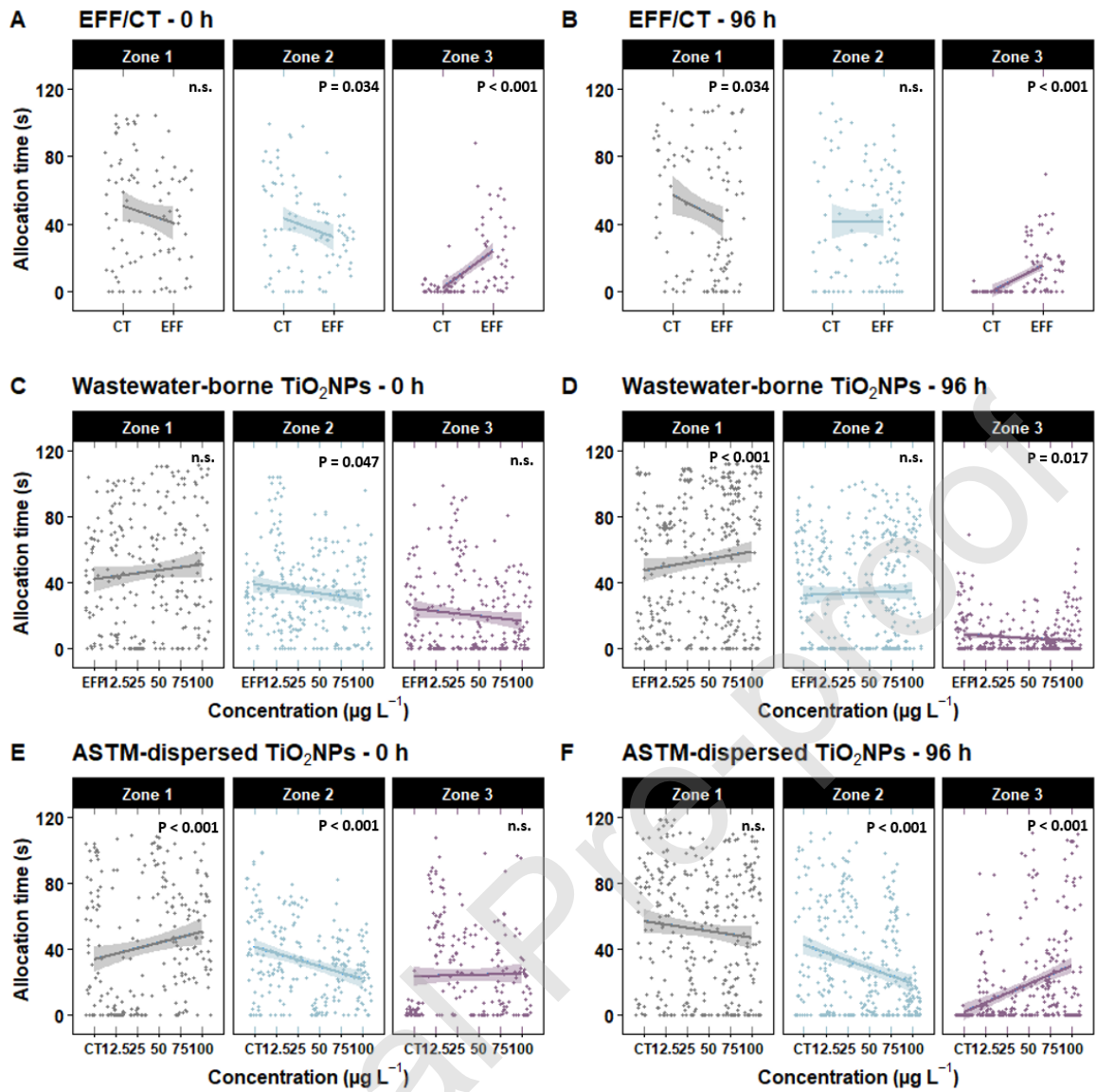


Fig. 8.

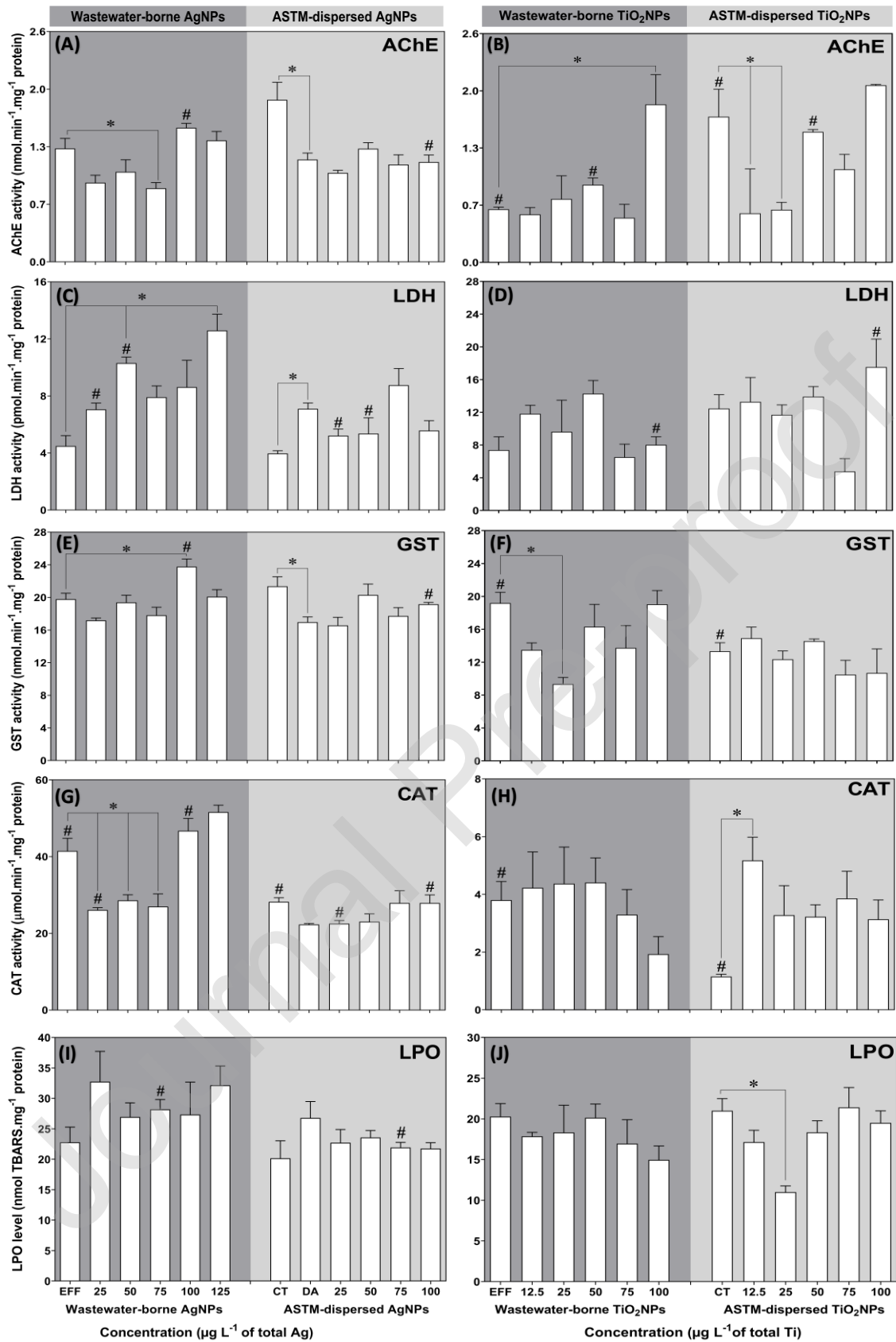


Table 1. Exposure experiments and respective treatments (test media + NPs), including controls, showing the nominal concentrations of NPs (in mg L^{-1}) supplemented to the WWTP influent and the dilution factors used for the preparation of tested concentrations in effluent (in $\mu\text{g L}^{-1}$) of total Ag and total Ti. EFF, CT, and DA are the controls (without NPs) composed by the effluent, ASTM medium, and dispersing agent, respectively. See text for further details.

Experiments	Treatments	WWTP: nominal sewage inlet concentrations (mg L^{-1})	WWTP: total concentrations in the effluent ($\mu\text{g L}^{-1}$) \blacklozenge	Effluent dilution factors (parts of effluent per parts of ASTM)	Nominal concentrations of NPs in the test media ($\mu\text{g L}^{-1}$)
1A	EFF *	0	n/d	1:1.2	0
	Wastewater-borne AgNPs	1	54 ± 3	1:2.1	25
		2.5	65 ± 2	1:1.2	50
		3.5	141 ± 3	1:1.8	75
		5	193 ± 3	1:1.9	100
		6.5	239 ± 4	1:1.9	125
1B	CT	n/a	n/a	n/a	0
	DA (ASTM medium + dispersing agent)	n/a	n/a	n/a	0
	ASTM-dispersed AgNPs	n/a	n/a	n/a	25
					50
					75
					100
				125	
2A	EFF *	0	< LOD	1:3.7	0
	Wastewater-borne TiO_2 NPs	1 [#]	104.3 ± 2	1:13.9	12.5
		1 [#]	104.3 ± 2	1:6.9	25
		2.5	114.1 ± 1	1:3.7	50
		5 [#]	464 ± 5	1:10.3	75
		5 [#]	464 ± 5	1:7.7	100
2B	CT	n/a	n/a	n/a	0
	ASTM-dispersed TiO_2 NPs	n/a	n/a	n/a	12.5
					25
					50
					75
					100

* The EFF controls served as stock solutions for the correspondent EFF controls used in the exposure experiments after dilution with ASTM medium. # In inlet with 1 and 5 mg L^{-1} TiO_2 NPs, two dilutions were prepared in order to achieve four different concentrations in the obtained effluents. In short, 6 + 4 WWTP units lead to 6 + 6 treatments, including controls, for exposure experiments with AgNPs and TiO_2 NPs, respectively. \blacklozenge Measured concentrations of NPs in collected effluents ($n = 1 \pm$ standard deviation of 10 and 3 internal replicates for total Ag and total Ti, respectively). n/d – not determined; n/a – not applicable; LOD – limit of detection.